STRUCTURAL SEISMIC RESPONSE CONTROL USING PASSIVE CONTROL DEVICES

Thesis

Submitted in partial fulfillment of the requirement for degree of

DOCTOR OF PHILOSOPHY

by

VAJRESHWARI UMACHAGI

(121173CV12F04)

DEPARTMENT OF CIVIL ENGINEERING

NATIONAL INSTITUTE OF TECHNOLOGY KARNATAKA

SURATHKAL - 575 025

SEPTEMBER 2020

D E C L A R A T I O N

I hereby *declare* that the Research Thesis entitled "**Structural Seismic Response Control Using Passive Control Devices"** which is being submitted to the **National Institute of Technology Karnataka, Surathkal** in partial fulfilment of the requirements for the award of the Degree of **Doctor of Philosophy** in **Civil Engineering**, is a *bonafide report of the research work carried out by me*. The material contained in this Research Thesis has not been submitted to any University or Institution for the award of any degree.

Vajreshwari Umachagi

121173CV12F04

Department of Civil Engineering

Place: NITK-Surathkal

Date: 04/09/2020

C E R T I F I C A T E

This is to *certify* that the Research Thesis entitled "**Structural Seismic Response Control Using Passive Control Devices"** submitted by **VAJRESHWARI UMACHAGI** (Register Number: **121173CV12F04**) as the record of the research work carried out by her, is *accepted as the Research Thesis submission* in partial fulfilment of the requirements for the award of degree of **Doctor of Philosophy**.

Research Guide

Dr. Katta Venkataramana
Professor
Department of Civil Engineering
NITK, Surathkal

Dr. K. Swaminathan
Chairman - DRPC
Department of Civil Engineering
NITK, Surathkal

ACKNOWLEDGEMENTS

I express my deep sense of gratitude to my thesis supervisor, Prof. Katta Venkataramana, for his unconditional support during my research study, his patience, motivation and constant optimism, which helped me immensely throughout my research.

I am grateful to my research progress assessment committee members, Prof. A. S. Balu, Department of Civil Engineering and Prof. B.R. Shankar, Department of Mathematical and Computational Sciences, for their advice, helpful insights and comments.

I would also like to thank Prof. K. S. Babu Narayan, Prof. M.C. Narasimhan and Prof. B. R. Jayalakeshmi, Department of Civil Engineering, for their support, encouragement and kind words.

My sincere thanks to Prof. K. Swaminathan, Head of Department of Civil Engineering, for his continuous support and encouragement. I also extend my gratitude to Prof. A. U. Ravishankar, Prof. K. N. Lokesh, Prof. D. Venkat Reddy and Prof. Varghese George, Department of Civil Engineering for their goodwill and moral support.

I thank my fellow research scholars, teaching, non-teaching staff and friends in the Civil Engineering department, for their motivation, help and support during my research.

I sincerely acknowledge the support by Bhabha Atomic Research Centre (BARC), Mumbai funding for project work to carrying out this research work.

My heartfelt thanks to Prof. G.R. Reddy, Head of Structures and Seismic Engineering section for his support and help to carry out this research work. I would like to thank, Shri. Rajeev Verma, Shri. P.N. Dubey and Dr. Y.M. Parulekar, for their support and helping me to complete my research work, senior scientist of Reactor Safety Division of Bhabha Atomic Research Centre, Mumbai.

My deepest gratitude to my family, for encouraging me to pursue my dreams and offering unconditional love and support during this journey.

Place: NITK, Surathkal **Vajreshwari Umachagi**

Date: 04/09/2020

ABSTRACT

In the present study, the seismic performance of R.C.C structure with X-plate damper (XPD) and superelastic shape memory alloy (SMA) damper is investigated. The combined effect of both XPD and SMA damper in the building is also considered. Metallic devices are made up of thin steel plates available in X or V shape triangular element, manufactured with mild steel or copper or aluminum material having thickness 2mm to 6mm. These devices work based on the concept that melting of metals through a loss of energy in the form of heat. Mechanism of X-plate damper involves energy dissipation in the form of heat, and it is effective technique during the earthquake to absorb the input energy of the structure. Metallic dampers utilize the inelastic deformation of metals and absorb the energy during vibration of structures. Similarly, shape memory alloys belong to a class of smart materials and are capable of regaining its original shape when subjected to heat at a specific temperature. Hence, SMA damper is used as energy dissipater and re-centering components.

In the present study, numerical investigation is carried out with nonlinear time history analysis of a three storeyed R.C.C structure equipped with XPD and SMA damper. The equivalent linearization and stiffness method are considered. In X-plate damper, the variations in the parameter, namely size (a=b=40mm and a=b=60mm) and thickness (t=3mm and t=6mm) of the steel plate and SMA wire diameter (0.4mm and 1.2mm) are also evaluated. The analysis results show that there is a decrease in the overall displacement of the building.

The results of analysis indicated that XPD, SMAD and combined effect of XPD and SMAD can effectively reduce the displacement of the structure during an earthquake. The XPD having thickness t=3mm and t=6mm with size of plate a=b=40mm is more effective compared to a=b=60mm. In addition, it is also noted that SMA having 0.4mm wire is effective compared to 1.2mm wire damper and is also more effective comparison with the XPD in the building. It is also observed that combined effect of XPD with size a=b=40mm and SMA wire diameter of 0.4mm is more effective compared to the higher thickness of the XPD. The results indicate that the utilization

of the proposed X-plate damper, SMA damper and combined effect of XPD and SMAD are effective in reducing the peak roof displacement and acceleration.
Keywords: Damper, X-Plate damper, SMA damper, Seismic performance

TABLE OF CONTENTS

LIST OF FIGURES

LIST OF TABLES

LIST OF NOMENCLATURE

Symbol	Description
a	Height of triangular portion
b	Breadth of triangular portion
d_y	Elastic depth
E	Modulus of Elasticity
E_A	Young's modulus of austenite
E_M	Young's modulus of martensite
F_y	Yield force
K	Equivalent stiffness
t	Thickness of plate
T	Temperature
Ts	Start temperature of transformation
σ	Stress
σ_y	Yield Stress
ε	Strain
s_{Ms}	Martensite start stress
s_{Mf}	Martensite finish stress
s_{As}	Austenite start stress
s_{Af}	Austenite finish stress
e_{Ms}	Martensite start stress
e_{Mf}	Martensite finish strain
e_{As}	Austenite start strain
e_{Af}	Austenite finish strain
α	effective coefficient of thermal expansion
ε_l	maximum phase strain
ξ	volume fraction of the martensite phase

CHAPTER 1

INTRODUCTION

1.1 General

In recent years, various structures across the world were unable to survive the severe earthquakes. A few countries experienced massive earthquakes namely viz., Northridge (1994) at California, Kobe (1995) at Japan, Koyna (1967) at Killari (1993) and Bhuj (2001) at India, are some of the earthquakes in the past that have caused major damages. During the earthquake, frequently we experience human loss, financial loss, and failure of man-made structures, major loss of infrastructure viz., historical monuments, industrial structures, bridges, roads, etc. In the past, various structures made of concrete and masonry were damaged or destroyed depicting they were vulnerable to seismic damage. Seismic events lead to structural impairments such as concrete buildings, steel structures, bridges, industrial buildings, and historical structures. Hence, it is required to develop seismic design of the building using new seismic technology with control devices to sustain earthquake is one of the major areas of research in the present scenario.

In conventional seismic design method, considering overall safety and to withstand building against earthquake, structures are designed and constructed to have sufficient strength and ductility of the building. The traditional design is quite expensive and not feasible. Earthquakes are the result of reduction in forces below the elastic level in the structure. To overcome this, Soong and Dargush (1997), suggested that in the past decade during the earthquake use of passive control technology resulted in reduction of seismic design forces on the building. In this method, control systems are used to control the motion of the structures or to modify it through some external energy supply. The vibrations produced by wind or an earthquake can be controlled without increasing the strength of the structure by placing passive devices, active control systems, and semi-active devices as they are part of structural control devices. A few benefits are high damping capacity, damping mechanism capacity for dynamic force, long service

life, ease of repair, low maintenance cost, and easy replaceability (Constantinou et al. 1998). To enhance the design, functionality, and safety of structures against earthquakes, passive control techniques are extensively used as they are reliable, have better control over response and are economical.

One of the popular techniques is advanced structural control technique which has become more popular tgo improve the response of the buildings under the wind and seismic event. There are four different categories of control systems viz., passive, active, semi-active, and hybrid control techniques.

Structural control systems can also be classified based on their dissipative nature. This technology finds many applications in retrofitting of existing structures and installation in new structures without affecting the structural characteristics of the building. Housner et al. (1997) studied the relation between control devices and other controlling theories of structural control systems.

Passive energy dissipation method is used as a protective system to improve the overall safety, maintenance, and stability of the structures during an earthquake. The passive energy dissipation devices consists of damping devices (friction damper and viscoelastic damper or viscous damper) or replaceable yielding metallic damper or tuned liquid damper as oscillators used for improvement in response of the structure under the effect of dynamic load, in the form of structural response reduction of the building, in the occurrence of earthquake and wind excitation (Soong and Spencer 2002).

1.2 Supplemental Control Devices

Supplemental control devices are also known as added control devices. Various supplemental control devices are passive devices, active devices, semi-active devices, and hybrid damper. These controlling devices can be operated by absorbing vibration energy, subsequently transmitted into the structures or to decrease the amount of energy which can be transmitted into the building.

The passive control devices do not require any external energy and this is one of the main advantages of these devices. Based on the forces developed within the passive

device, dissipation of energy demand on the structure is reduced by absorbing some of the input energy.

In active control systems, sensors are attached to the structures with the supply of the external load or power supply. The active control devices provide supplementary energy to the controlled structure in comparison with the passive control devices studied by Soong (1990).

The semi-active devices are defined as the combination of two or more than two types of control systems. The combination of two different elements i.e., active systems and passive devices require lesser force or power supply when compared to active control systems, and they are operated based on sensors (Symans and Constantinou, 1999). Particularly, these active devices and semi active control devices can be used during high wind and strong earthquakes. However, like an active damper, the design properties of semi-active systems are adjusted based on the feedback controlling excitation (Spencer and Nagarajaiah, 2003).

The hybrid control device is a single device and it consists of a combination of two dampers having different material properties, i.e. passive devices and active devices, passive damper and semi-active devices and active and semi active devices (Soong and Spencer, 2002). Development of an appropriate seismic control devices theory to produce efficient and effective control device is required.

The control systems such as active, semi-active and hybrid dampers are related to the passive control systems. In the last few years, the combination of two dampers like passive-passive devices, active-passive device or passive and semi-active devices known as hybrid devices have gained considerable attention in seismic control of structures subjected to an earthquake.

In the last few decades, the research program was initiated at the National Institute of Standards and Technology, to develop the guidelines for testing of passive and supplemental devices. Based on the performance of structural control systems under static and dynamic loading for the reduction of response building and availability of standards for evaluating and testing the devices, previous researchers recommended guidelines for the design and construction of structures and have been widely accepted.

These guidelines are useful for the appropriate design and construction of structures with damping devices.

Michael et al. (1999) illustrated the schematic representation of different types of energy dissipation system namely, passive systems, active systems, and semi-active systems and also explained the concept of structural control into practical design, specification and construction of the building, many such control systems are installed in different types of structures like bridges, industrial steel building and midrise residential building etc.

1.3 Passive Control Dampers

Addition of passive devices to structures for vibration suppression concept was proposed by Soong and Dargush (1997). These devices developed the forces at the place/site of building utilizing the movement of the structures. Passive control systems reduce the energy dissipation demand on structures through forces developed on the structures by input energy-absorbing technique. Thus, it was established that passive devices do not add extra energy to the structural system. Further, for passive control systems, the extra amount of power supply is not necessary in comparison with the active systems and semi-active systems. But, in case of severe earthquakes due to frequent power failure, active devices and semi-active systems cannot operate. Thus, it was suggested to go for passive devices. Passive control devices act according to the response of the structures and reduce the structural response.

In the past literature, several devices have been proposed such as base isolation, viscous damper, viscoelastic damper, X-plate damper, tune mass damper, friction damper, shape memory alloy devices and lead rubber bearing and combination of these devices. Also, it is found that the metallic and shape memory alloy dampers are effective to reduce response of the building, easily attached to the structure, easily replaceable devices after the earthquake, repairable and widely accepted in civil engineering applications and their implementation in the construction of new building and retrofitting of the old building.

1.4 Scope of Research

The seismic performance of reinforced concrete R.C.C structure with X-plate damper (XPD) and superelastic shape memory alloy damper (SMAD) is carried out in the present study. In a building, the combined effect of both XPD and SMAD is also considered. Shape memory alloys is classified under smart materials, capable of regaining their initial shape when subjected to heat at a certain temperature. Hence, SMAD is used as an energy dissipator and re-centering component. Numerical modelling is carried out with nonlinear time history analysis of a three-storeyed R.C.C structure equipped with XPD and SMA damper and combination of XPD and SMAD is done. The equivalent linearization stiffness method is adopted in this study. In XPD, the parameters varied are size and thickness of the steel plate. The integrated three-storeyed R.C.C structure is analysed by finite element software, ANSYS version 16.0, considering linear elastic behaviour of the structure. The finite element analysis is performed for the building with damper (XPD, SMAD and XPD & SMAD) and without damper.

The seismic analysis of the integrated three-storey R.C.C structure is carried out with ground motions in the time domain. In the present seismic analysis of the building, the Rayleigh damping is assumed and the acceleration of available time history data is applied to the complete structure model in the global X-direction. The mass of the building and stiffness are proportional to equivalent damping i.e. 5% of critical damping is assumed as structural damping. The responses in the building such as lateral displacement and acceleration responses are evaluated for both the cases as mentioned above for the buildings with damper (XPD, SMAD and XPD & SMAD) and are compared with that obtained from the conventional analysis. A simplified design procedure is proposed that enables the structural engineers to determine the seismic response of building under the influence of damper, utilizing the fixed base analysis results as well as the other basic site condition and structural characteristics.

1.5 Objectives

The objectives of the research study are,

1. To investigate the dynamic behaviour of structures equipped with passive dampers such as X-plate yielding damper and SMA damper under seismic excitation.
2. To compare the response of building, X-plate damper with shape memory alloy damper under seismic excitation.
3. To evaluate the dynamic response of structures under the combined effect of passive dampers subjected to earthquake excitations.

1.6 Organization of the Thesis

Chapter 1 contains a brief introduction about passive control devices and their uses to control the buildings during an earthquake. The aims, objectives, and scope of the present work are also stated.

Chapter 2 covers a detailed literature review of previous studies related to the effectiveness of X-plate damper, SMA damper and hybrid damper in the building and also includes discussion on the literature about the present study.

Chapter 3 presents the formulation of dampers. It also includes the methods for the seismic performance of buildings with dampers.

Chapter 4 presents the numerical analysis of building and methodology followed. It also includes the seismic performance of a building under significant parametric variation of damper properties.

Chapter 5 discusses the results obtained from numerical methods of seismic performance of a building under earthquake with dampers i.e. XPD, SMAD and XPD & SMAD and without dampers.

Chapter 6 covers the main conclusions drawn from the present study and suggestions for future work.

CHAPTER 2

LITERATURE REVIEW

2.1 General

This chapter deals with the literature review on X-plate damper (XPD), shape memory alloy damper (SMAD) and hybrid damper related to the study undertaken in this research work.

2.2 X-Plate Damper (XPD)

Soong and Spencer (2002) proposed the elastoplastic dampers (EPD), which are also known as hysteretic dampers, since they possess desirable properties like being a stable hysteretic behaviour, short fatigue life, long term reliability are used for seismic protection of buildings. Thin steel or metallic plates available in X or V shape triangular elements are used to manufacture these devices. X-plates are available at different thicknesses: 2mm to 6mm and made using mild steel or copper material. During the seismic event, energy-dissipating mechanism of XPD provides adequate energy dissipation capacity; it will absorb the input energy of the structure. The metallic substance of the steel plate deforms inelastically by utilizing the input energy and also absorb the energy of the structure during seismic excitation of the building. Kelly and Skinner (1972) suggested a new metallic X and V-shaped energy dissipating devices. These devices were found to be efficient methods for absorbing the input energy due to plastic deformation of the metal plate. In the early 1990s, mild steel with X shaped plates were proposed since the strain in the device remained constant over the height of the device. These devices are also known as added stiffness devices (ADAS) and triangular shaped devices (TADAS) (Whittaker et al. 1991 and Tsai et al. 1993).

Wen et al. (1980) predicted the hysteretic curve of X-plate damper using the equivalent linearization technique. Whittaker et al. (1989) suggested the codal design procedure for the design and implementation of the X-plate damper. Whittaker et al. (1991) conducted experiments on steel plate ADAS element under the dynamic loading. The parametric study of the ADAS element used as supplemental device in the building was proposed by Xia et al. (1992). Several experimental tests were conducted on the passive energy device by Aiken et al. (1992).

The mathematical modelling of ADAS devices was proposed by Tena-Colunga (1997). Namita et al. (1991) conducted experiments on piping systems under dynamic loading conditions by replacing the snubbers with the yielding metallic damper. Tsai (1995) developed the mathematical models for triangular (tapered) plate energy absorber, based on a plastic theory using a finite element formulation.

Caughey (1960) proposed a new theoretical method, i.e., equivalent damping and stiffness method. This method was utilized to control the vibration of the piping system during strong ground motion. The equivalent stiffness of a single degree of freedom of a piping system with bilinear hysteretic characteristics of the damper was considered as a function of the amplitude of the displacement. Park et al. (1995) adopted a similar type of foregoing functions to express metallic devices. Reddy et al. (1999) studied the actual seismic performance of the piping system with the friction damper under seismic event using the equivalent damping and stiffness method. Parulekar et al. (2004) extended the same equivalent damping and stiffness method for the response control of the coolant channel model supported with lead extrusion damper under seismic excitation.

Tehranizadeh (2001) conducted numerous experiments on single added damping and stiffness devices (ADAS) to resist the seismic forces in a steel building. It was concluded that these elements sustain more load at large deformation and suggested a new device design approach to improve the seismic response of building subjected to an earthquake.

Satishkumar et al. (2003) performed experimental and analytical studies on the passive yielding dampers also known as X-plate damper or elasto plastic damper as shown in Figure 2.1. The Ramberg-Osgood and Power-law methods were studied to provide the connection between the force and the inelastic displacement of the steel plate. To check the response and modelling of the steel plate under cyclic dynamic loading, the power-law method was used. These devices were designed to absorb the input vibration energy through inelastic yielding of metallic elements. To analyse the effectiveness damper, yielding dampers were installed in the piping system subjected to a seismic event. Interpretation was made such that the yielding type of metallic dampers reduce upto 40% of seismic response in the piping system when subjected to earthquake.

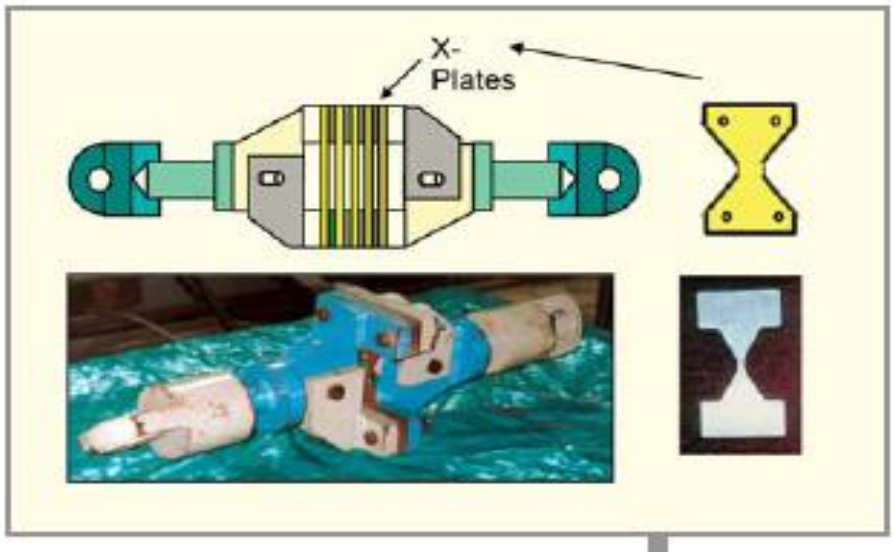

Figure 2.1 X-plate damper (Satishkumar et al. 2003)

Curadelli and Riera (2004) suggested the new metallic devices for seismic retrofitting of the building. Ten-storeyed steel building and six-storeyed reinforced concrete building with metallic dampers were analysed using reliability-based method to provide external energy dissipation to the buildings. Experiments were conducted to generate the mechanical properties of the lead ring damper. The results show that, the possibility of failure of both structures was between 70% and 80%. The external energy dissipation system is a useful technique in reducing the dynamic response of the structures.

Parulekar et al. (2006) studied the elastoplastic passive energy dissipation devices to reduce the seismic vulnerability of the pipeline system during artificial seismic ground motion. In this study, snubbers were replaced by elastoplastic dampers. The linear and nonlinear time history analysis and equivalent linearization techniques and procedure were applied to determine the peak displacement of the piping system with elastoplastic damper subjected to dynamic loading. The testing of SDOF cantilever piping was conducted on the shake table subjected artificial time history acceleration data. Time history analysis was carried out with a 3mm thick plate attached to the piping system and without including 3% damping for 0.15g, 0.45g and 0.9g peak acceleration on the piping system. Experimental results were correlated with the analytical results. The analysis depicted 40% reduction in the response with less than 10% change in frequency of the piping system.

Bakre et al. (2006) investigated effect of XPD in piping systems under seismic event. Using an incremental step by step of Newmark's time-stepping method and with varying properties of XPD, the time history analysis of piping system with XPD was performed using real earthquake data. It was concluded that, the amount of energy absorbed by XPD in the piping system equipped with XPD is increased due to the hysteretic behaviour of XPD. Based on the obtained optimum properties of XPD, there is a significant response reduction in the piping system.

Parulekar et al. (2009) studied regarding retrofitting of R.C.C structures using the elastoplastic damper under earthquake load. Experiments were conducted considering a three-storeyed, two bays R.C.C frame structural model with and without elastoplastic damper attached to the frames. The equivalent stiffness for a bilinear hysteretic characteristic of SDOF building system is given as a function of the amplitude of the relative displacement. The experimental results were compared to the analytical results and resulted in good agreement.

Pujari and Bakre (2011) studied the seismic response of the structures with XPD provided at different locations of the square-shaped multi-storeyed building. To identify the optimum location of XPD in the building, the objective function was selected considering the linear combining inter-storey drift and base shear of the building. The XPDs are placed at different locations of the building. The building frame was analysed using SAP2000 software with XPD at all bays were considered. The numerical time history analysis results show that, there is decrease in the response of the building was observed and concluded that the optimum location of XPDs in the building was found to be effective.

2.3 Shape Memory Alloy Damper (SMAD)

Shape memory alloys are smart materials capable of retaining their original shape when heated to a specific temperature. Previous researchers on SMAs have been reported to increase its effectiveness in commercial products. The SMA damper is used in the control system of buildings, bridges, etc. Ni-Ti alloys are commercially available alloys. The Ni-Ti alloy having larger strain recovery capacity (upto 8%), is thermally stable, has good corrosion resistance and higher ductility. Because of these properties, SMA devices are suitable for vibration control of structures. The first shape memory's transformation and the metallographic phenomena and resistivity changes were observed in Aurum Cadmium alloy (AuCd) proposed by Chang and Read (1932). Later, the same shape memory effect was observed in nickel-titanium alloy and it is known as Nitinol. Graesser and Cozzarelli (1991) proposed one-dimensional stress-induced micromechanical phase transformation process to achieve large hysteretic deformation in SMAs due to the hysteresis behaviour, associated with phase transformation.

In dynamic applications on structures, the SMAs show a greater potential for use as a passive damping device. Since then, various types of SMA damper devices have been discovered. Among different types of alloys, one of the most commonly used SMA alloy is Nitinol, which has very superior thermomechanical and thermo-electrical properties. Generally, these materials get deformed at a lower temperature and regain their original shape by heating to some higher temperature before going to the

deformation. The shape memory effect and the superelastic effect are the two main properties of SMAs. The reversible phase transformations of SMA is the effect of these two unique properties. There are two crystal structure phases in SMA, namely the austenite and martensite structure phases stable at high and low temperatures, respectively. Martensite SMAs possess a high damping capacity compared to austenite by having the large re-centering force to recover the structure to its initial position with a small quantity of residual strain.

The thermoplastic martensite yields the martensitic transformation, and it develops the austenite phase at the longer duration and higher temperature in shape memory alloy. In the first phase transformation with a single temperature, there is no change in the alloy; gradually, there is a change in temperature observed. At higher temperature, heating or cooling process takes place, but at a relatively low-temperature range, SMA exhibits hysteresis characteristics which do not overlap during the heating and cooling process. Certain shape-memory alloy wires regain its shape until heated above transition temperature and in its cold form wire can be bent or stretched known as one-way shape memory alloy and other metals show a shape-memory effect both during heating and cooling known as two-way shape memory alloy. The two different types of SMAs available are nickel-titanium and copper-base alloys such as Cu-Zn-Al and Cu-Al-Ni, which can be further classified based on thermoplastic martensite characteristics as martensite and austenite phase transformations. Martensite variation shows reorientation and stress-induced martensitic transformation, whereas austenite shows the superelastic phase transformation. The Ni-Ti alloys up to 8% greater shape memory strain are thermally stable and have good corrosion resistance. The copper-base alloys have more potential transformation temperatures, can be melted and extruded in the air with ease and are less expensive. On the other hand, copper-based alloys have medium corrosion resistance, only 4% to 5% strain, susceptibility to stress-corrosion cracking and very high ductility compared to NiTi alloy (Darel 1990).

In NiTi alloys, lower the transformation materials are iron and chromium. Similarly, copper is used to reduce the deformation, stress of the martensite, and to decrease the hysteresis. The mechanical properties of SMAs degrade because of existing contaminants such as oxygen and carbon that can shift the transformation temperature. Hence, it is also necessary to minimize the quantity of these elements. The NiTi alloy based SMAs are efficient passive vibration suppression devices comprising hysteretic dampers with the unique characteristics of Young's modulus, shape memory effects, temperature-dependent and high damping capacity, which makes them useful as devices for seismic-resistant design and retrofit. Experimental and analytical investigation of superelastic NiTi alloys shows that, they are efficient and attractive for seismic by improving the design and the response of building and bridges subjected to an earthquake.

2.4 General Characteristics of SMA

Several researchers have reported experiments conducted to understand the mechanical behaviour of SMA bars and wires. Large number of literature available on shape memory alloy wires compared to another different form of SMA wires and bars. The past research indicated that, SMA wire has more superelastic property compared to SMA bars and in any other form of SMA. The cyclic behaviour of SMA wires and bars with different diameters from 1.8mm to 25.4mm have shown acceptable recentering capabilities with a different constitutive model. The authors concluded that, the SMA wires showed more strength, superelastic property and damping compared to large diameter bars. Other researchers investigated that, by adopting a suitable quantity of chemical composition, heat treatment and deformation, the larger diameter bars show the same strength and superelastic property of SMA wires (Desroches et al. 2004 and Jason et al. 2006).

The capability of a material to absorb or release the vibrational energy of structure by transforming mechanical energy into heat energy is known as damping capacity. The damping capacity of SMAs material is related to the hysteretic moment of the martensitic variant interfaces and the equivalent viscous damping ratios of SMA

material attained its maximum up to 4-5% of the cyclic strain level and reduced beyond that strain level. The study also indicated that damping ratios were 4%-8% for wires and 2%-4% for bars, which shows that SMA wires have higher equivalent viscous damping compared to SMA bars (Desroches et al. 2004). Mccromick et al. (2006) studied regarding SMA wires of 0.254mm diameter under quasi-static tension loading, the results demonstrated a higher equivalent viscous damping of 5.3%, while 12.7mm NiTi diameter wire showed 2.7% equivalent viscous damping. Similarly, a study by Mccromick et al. (2007) showed that, for 12.7mm diameter SMA bar, equivalent viscous damping was 30% higher than that of 19.1mm diameter bar and concluded that the residual displacements slightly increased with larger diameter SMA bars.

The properties of SMA wire are discussed in the following sections.

2.4.1 Cyclic properties of SMA

Earthquake events induce cyclic deformation. To understand the cyclic behaviour of NiTi SMAs under seismic event, various researchers conducted experiments on NiTi SMA wire subjected to repeated cyclic loading with incremental strain levels. Few researchers investigated the superelastic property of NiTi SMA wire and bars and conducted the experimental tests to study the influence of repeated loading, fatigue and under cyclic loading conditions (Desroches et al. 2004, Dolce and Cardo 2001). The test results showed that, an increase in the number of loading cycles increases the residual strains while loading plateau stress level and hysteric loops decrease. Also, variation in the forward phase transformation was observed under different stress levels. To achieve stabilization in the hysteric behaviour of NiTi wires, researchers investigated greater number of cycles trained on NiTi wires. The NiTi wires provide stable flag-shaped hysteric behaviour by training NiTi wire approximately up to 20 cycles (Mccormick and Desroches 2006, Wang et al. 2003). Desroches et al. (2004) observed small levels of localized slip due to the maximum cyclic behaviour variation of SMA wire in the first and second cycles. Also, the cyclic properties of superelastic SMA wires and bars were studied by varying the sizes and loading history. Malecot et al. (2006) studied the cyclic tensile test of NiTi SMA wires having 2mm dia, indicating

that, due to variation in stress-strain curve the variation in cyclic behaviour in the forward transformation of wire is observed. Mccormick et al. (2007) conducted an experimental investigation on large diameter NiTi bars of 12.7mm, 19.1mm, and 31.8mm, while Wang et al. (2016) proposed the real scale test results of large diameter superelastic NiTi SMA bars varying from 8mm to 30mm.

Moreover, other researchers investigated the cyclic behaviour of NiTi wires (Dolce and Cardone 2001, Zhang and Zhu 2007, Dezfuli and Alam 2013, Parulekar et al. 2014). The test results indicated similar degradation of NiTi wire and bars under cyclic load. In the recent study, researchers conducted experiments on the superelastic behaviour of SMA cables. These cables are made by assembling several strands laid helically around the central core. The SMA cables offer unique characteristics such as superior performance than SMA large diameter bars, new adoptive functionality, super elasticity and shape memory effect (Reedlunn et al. 2013, Carboni et al. 2015, Ozbulunt et al. 2015). In general, based on the design flexibility, SMA wire provides large tensile stiffness and strength. They are relatively damage resistant and fatigue resistant, since the failure of a single wire in a multi-wire cable provides redundancy, unlike the sudden fracture in a larger diameter monolithic bar.

Reedlunn et al. (2013) discussed that SMA cables have superior mechanical properties, large force capacities and lower cost over SMA bars. Due to these properties, SMA cables can be used in the application of the superelastic effect in infrastructure. The study also included the hysteretic characteristic of the single SMA wire and group of SMA strand and observed that at the same strain level the restoring stress of the strand is less than that of the single SMA wire.

2.4.2 Strain rate effect of SMA

Azadi et al. (2006) studied that their loading rate significantly influences the mechanical behaviour of NiTi SMA. During the phase transformation, the rate of loading behaviour of SMA wire depended upon the effect of temperature, the rate of heat generation and the interaction between stress. The test results demonstrated that, some amount of latent

heat is generated or absorbed during martensitic reversible phase transformation (He and Rong 2004, Liu and Huang 2006). The experimental results indicated that, the SMA material required adequate time to exchange phase transformation induced latent heat to the environment. However, insufficient time was available during loading with high strain rates to transfer the heat in that process. Therefore, during forward transformation, the temperature of the SMA material altered and modified the shape of the hysteresis loops and transformation stresses. In civil engineering structures, under the dominant frequency range of 0.2Hz to 4Hz during the seismic event, the rate of loading influenced the mechanical response characteristics of NiTi SMA. Before the actual implementation of NiTi SMA in civil engineering structures, the loading effect on the superelastic behaviour of NiTi SMA is an important consideration in evaluating its mechanical characteristics. Since the SMA material encounters dynamic effects during a seismic event, the increase in the loading frequency and consequently the strain rate, increases the loading plateau and decreases the amount of the hysteretic damping of NiTi SMA (Dolce and Cardone 2001, Desroches et al. 2004).

In the past literature, it was found that there is inconsistency in findings the effect of loading rate caused by multiple factors such as, different composition of the material, experimental testing at different strain rates and test conditions. When the strain rate increases, the reverse transformation stress is also increased, without the considerable variation in the forward change in stress, but the energy dissipation is decreased (Wolons et al. 1998 and Ren et al. 2007). Similarly, previous researchers studied that, the increase in strain rates contributes to an increase in both forward and reverse stresses. Moreover, it was noticed that the higher strain rates attribute to increase in forward transformation stress and decrease in reverse transformation stress (Tobhushi et al. 1998).

2.4.3 SMA wire-based dampers

Zhang and Zhu (2007) investigated the recentering hybrid damper (RHD) is an SMA-based reusable hysteric damper in the seismic control of structures subjected to an earthquake event. The RHD was developed to provide distinctive features, such as the

tuneable hysteric behaviour and its ability to withstand several design-based earthquakes by utilizing the dissipation of energy through the superelastic NiTi wire. The design parameters of RHD are, the inclination angle of SMA wires, pretension levels and friction coefficients of the dampers adjusted to achieve the suitable hysteretic behaviour of the damper. The hysteric behaviour of RHD device was validated through the experimental results, and an analytical model of the same was developed to predict its response. Three-storeyed steel building with RHDs was considered for the numerical simulation and it was concluded that, RHDs were useful to reduce the response of structures and it acts as a passive control system during an earthquake.

The dynamic behaviour of the building frame was equipped with an SMA wire-based passive control device. Experimental investigation was conducted on properties such as durability, fatigue resistance under large strain and reliability. The results illustrated that, SMA devices absolutely upgrade the dynamic response of the building structure (Dolce et al. 2000, Baratta and Corbi 2002).

Saadat et al. (2002) studied the unique thermomechanical behaviour of the NiTi SMA design, modelling an overview of its application and included the vibration applications of NiTi SMA wire devices in the civil engineering field.

Tamai (2002) proposed the experimental investigation of SMA wire. To understand the restoring force properties of the SMA nitinol wire, a tension loading test at different temperature was conducted. Experimental results were used for implementing the SMA wire as a hysteretic damper for vibration control of buildings.

Yu Lin et al. (2003) investigated the SMA wire-based device for seismic control of structures. In this study, the vibration reduction of the steel frame of 2m height is analysed by implementing the SMA wire-based device. Free vibration analysis of building frame was carried out with and without SMA device using the finite element method. The experimental and numerical analysis results illustrated that the proposed SMA damper is effective in reducing the structural response of buildings.

Justin et al. (2004) investigated the SMA bar in connection with the beam-column joint. The column to column connections consisted of four large-diameter NiTi SMA bars of size 381mm long with a diameter of 35mm in the central gauge length of 229mm. The beam flange to the column flange connecting ends of the bars diameter of size is 44mm. Results showed that, energy dissipation from the SMA bar fixed in the beam-column joint connection was very high. Subsequently, the presence of SMA bar subjected to cycles, increased drift level-up to 4%.

Hashemi and Khadem (2006) investigated the behaviour and specification of NiTi shape memory alloy, presented a simple and suitable mathematical model. Auricchio model was used to understand the superelastic behaviour of SMA in the phase transformation processes like austenite and martensite state with various elastic modulus and temperature effects. To check the efficiency of the developed model, simply supported and free clamped condition of the beam with SMA was analysed. The beam is subjected to dynamic loading conditions with a variation of elastic modulus and temperature effect. The presence of the elastic module in different phases caused a change in system stiffness due to variation in natural frequencies, which led to an escape from resonance.

The design and analysis of steel building and SMA braced frame structures are subjected to seismic excitation are compared. The bracing systems were provided at different locations of the building in the form of diagonal, split X, chevron bracing system. The various types of SMA dampers were implemented in the structure as a bracing system to reduce the seismic response of the building during an earthquake. An analytical study was carried out on the building frame with SMA bulking restraint as a bracing system. The effect of pseudo-elasticity and reorientation of martensite SMA damper were observed (Motahari et al. 2007, Jason et al. 2007, Matthew et al. 2009, Chuang et al. 2010, Asgarian and Moradi 2011, Mohamed 2014). Results showed that the behaviour of different types of SMA braces improved the dynamic response of the structure as a residual deformation in the seismic response reduction during seismic excitation.

Torra et al. (2007) demonstrated the damping capabilities of the SMA for building structures. The results revealed that the proposed system reduced the maximum amplitude of earthquakes and dissipated 50% of the energy absorbed by the structure. An innovative passive control SMA device was designed and implemented in cable-stayed bridge model (Charney et al. 2008, Sharabash and Andrawes 2009). The SMA device was attached to the bridge at the deck tower and pier for the seismic control of the structure. Assumed damping factor of 2%, the model analysis of the bridge was carried out using OpenSEES software. The comparative study shows that, with the introduction of the SMA damper in the bridge, there was significant reduction of displacement compared to the response of the conventional bridge.

Russell et al. (2010) investigated the SMA restrained cable provided in the limiting hinge opening in the bridge. The SMA cable was tested equipped in concrete slab bridge subjected to seismic ground motion. The experimental test results demonstrated that, the SMA cables reduced the bridge hinge openings and the column drifts by 52% and 47%. The FEM model of the concrete slab bridge with SMA restrained test setup was developed. The numerical analysis results showed that the SMA cables reduced the hinge openings by 69%.

Qian et al. (2013) investigated the SMA based damper for seismic protection of buildings. In this study, the improved constitutive equations of the Graesser and Cozzarelli (1991) models were used. The effectiveness of the proposed model for a ten-storey steel frame with and without SMA dampers were analysed using nonlinear time history analysis. Results showed that, the superelastic property of SMA wire was useful for the seismic control of structures during an earthquake.

2.5 Hybrid Dampers

The concept of using new materials in terms of combined control strategy has become more popular in the field of civil engineering. The hybrid damper is a single device made up of two different combination of two dampers or two different dampers in one single system for example, base isolation with tuned mass damper, base isolation with

tune liquid damper and viscoelastic and friction damper in a building structure. Based on this concept, the combination of using two devices with different material property, making new devices, i.e. hybrid devices, became worldwide. From recent research it is found that hybrid device is effective in reducing the overall seismic reduction response of the structure under seismic excitation.

Performance of the structure under earthquake load is observed with combined control strategy of TMD with a base isolation system. Numerical models were tested and simulated with and without TMD subjected to seismic excitations by stationary Gaussian random processes. Results showed that, combined effect of base isolation and TMD were efficient in reducing the seismic excitations of overall system response in the presence of nonlinear behaviour of the isolators and also systems isolated at the base with low damping and equipped with TMD placed at the top of the building to understand the seismic performance of the structure (Kareem 1997).

Bhasker and Jangid (2001) investigated the laminated rubber bearing with steel plates and a sliding bearing based base isolation system. A series of experimental tests were conducted to determine the response of structure supported on the base isolation system under harmonic excitations. Results indicated that the isolation devices were effective in the seismic response reduction of structures.

Caracoglia and Jones (2007) investigated the passive hybrid systems. The retrofitting of inclined cable-stayed bridges with the combined effect of cross ties and external dampers were considered in which the bridge was frequently affected by wind-induced vibration excitation. In this study, Fred Hartman cable-stayed bridge was selected in which cross ties and dampers were connected to the deck of the bridge. During wind excitations, a large amplitude of vibration was observed in the stayed bridge. Due to these 12-cable configurations were modified into three groups of cross ties and external dampers were attached to the system. For simulation purposes, the equivalent model was developed in which each cross tie was simulated as a linear spring with reference to the first cable frequency AS1 as f_{01}=0.625Hz. Further, the analysis of the network was carried out using two external viscous dampers. Critical damping was calculated

numerically and it was found out that D1 and D2 were approximately 4.3 and 3.1 respectively. Results showed that hybrid damper significantly improved the bridge deck under wind excitation.

Torra et al. (2007) investigated the SMA dampers using the phase metastability property. The damper was developed using a shape memory alloy effect and thermodynamic force of phase transition actions was considered. In the building frame, the SMA damper is placed in a diagonal pattern and beam structure. The building frame with SMA dampers are modelled and the FEM analysis was carried out using ANSYS software under the available earthquake data. The dynamic response of the structure was obtained using a simulation technique. Results demostrated that the SMA damper reduced the oscillation amplitude to the half and in the 1^{st} and 2^{nd} floor the maximum peaks were reduced to 3.0 cm and 7.1 cm.

The SMA-based bracing system in the steel building using combination of self-centering and friction devices (SFBD) was analysed (Zhu and Zhang 2008 and Song et al. 2008). The dynamic analysis of three and six-storey steel concentrically braced frames (CBFS) were conducted for a comparative evaluation of SFDB frames and buckling restrained braced (BRB) frames subjected to ground motions. The result demonstrated that SFDB frames could provide a comparable seismic response to that of BRB frames, in terms of peak inter-storey drift, while reducing the residual drift considerably. Further, the results highlighted the enhanced seismic performance of the SFDB due to the potential benefit of the frictional damping in the device.

The two-phase hybrid passive control device (HPCD) was considered to mitigate the seismic performance of the steel structure developed (Marshall and Charney 2010a, Marshall and Charney 2010b). It was designed using high damping rubber with steel buckling restrained braces. HPC device was tested cyclically and statically when subjected to an earthquake. It consists of a rubber damper with buckling restrained braces. Material testing was conducted at various frequencies of 0.5Hz, 1Hz, 2Hz, 4Hz, and at different strain levels. It is indicated that, the material samples were statically deformed to the desired range until steady-state static property produced up to 10

cycles. Based on test results, a numerical analysis was carried out on a hybrid device. The device was modelled with NR60 and BR60 materials and steel components were modelled using 250MPa yield stress and 400MPa ultimate strain with 0.2 plastic strain. To evaluate the response of the device, a set of sinusoidal displacement test was conducted. Later, the nine-storeyed building was considered to check the performance of the HPCD under seismic records. Finally, HPCD shows good response to reduce the seismic response of the structure during a seismic event.

The seismic performance of bridge with a combination of SMA-based devices and a sliding-type base isolation system was proposed under environmental temperature condition (Ozbulut and Hurlebaus 2010, Osman and Stefan 2010). SMA-based isolation system strategically combined a steel Teflon sliding bearing applied to dissipate energy through frictional behaviour and NiTi SMA wires were used to offer additional energy-dissipating and re-centering capabilities. The neuro-fuzzy model was considered to understand the behaviour of superelastic NiTi wires at different loading rate and temperature range. To calculate the length and area of SMA wire, a genetic algorithm tool was used. To determine the seismic response of a multi-span isolated bridge at the various outside temperature, a sliding bearing with an SMA damper was installed. The results indicated that, the changes in the temperature are a moderate effect on the performance of an isolated bridge structure. Particularly, the result highlighted that when the temperature changes were around 200^0 C, there was 13% variation in the displacement and 8% variation in the acceleration in response of the bridge. The SMA based isolators are effective in controlling the structural response of isolated bridges under seismic event. To protect the bridges against near-fault earthquakes, the SMA/rubber based (SRB) devices are very useful. In the SFBI system, the SMA wire device acts like a recentering device and the energy dissipated through friction damper. In the SRB isolation system, the SMA damper dissipates energy in the form of hysteretic energy, so it requires a very large amount of SMA material. Finally, SFBI had more desirable properties compared to SRB isolation system.

Yang et al. (2010) investigated hybrid devices with SMA wire, which provided the dual characteristics of energy-absorbing and re-centering capabilities, to mitigate the structural response during seismic events. The hybrid damper consists of three components such as a set of re-centering SMA material, two energy-absorbing struts, and two high-strength steel tubes are provided. The length of the SMA wire was designed in such a way that their strain outcome was expected to be within the target strain of 6%. This limitation indicated full re-centering capability and the SMA stiffening phase even in the occurrence of large deformations. To avoid the buckling issue while compression loading, the energy-absorbing struts were designed for a seismically compact and stocky. To explore the behaviour of structure with hybrid SMA damper numerically, three storey SAC building was analysed. The SMA damper was installed in different configurations in the frame between a beam and braces placed horizontally and simple like diagonal elements. The numerical study results concluded that, the SMA-based hybrid dampers contributed higher performances compared to the BRB frame in energy dissipation capacity and peak inter-storey drift, which also indicated superior re-centering capabilities.

Toopchi Nezhad et al. (2011) investigated the seismic performance of the building with the effect of tuned mass liquid damper (TLD) and base isolation dampers in the building. The modelling of both TLD and base isolation was based on equivalent linearized mechanical technique and Bouc-Wen model. The preliminary parameters of the TLD are appropriate dimensions of the tank and damping properties were designed. The model was validated with time simulation procedure and the fluid in the tank was accounted for the nonlinear behaviour of the structure. The TLD and base-isolated structure was found to be effective means to control wind and seismic response of the building.

Qian et al. (2013) investigated the innovative devices called recentering shape memory alloy damper (RSMAD) to mitigate the seismic performance of the building. The RSMAD was designed using superelastic NiTi wires as energy-dissipating elements. The improved constitution model for SMA wire was used, which is developed by Grasesser and Cozzareli (1991) and validated by the cyclic tensile compression tests on

the SMA damper. The test was conducted under various loading frequencies and displacement rate at different pre-strain values. It is observed that the experimental results validate the hysteric behaviour generated. Based on the improved constitutive model, the good martensitic hardening features of SMAs under large amplitudes, with a superior performance both in the re-centering and energy-dissipating characteristics under different loading conditions were observed. In the numerical simulation, a ten-storey building with a newly proposed SMA damper was evaluated under earthquake excitation. The simulation results showed that, the SMA based dampers were capable of significantly reducing structural vibrations.

Wilson and Wesolowsky (2013) proposed the performance of isolators with the SMAs in the building. For designing isolators, conventional methods were used and the period shift and damping values are found out. To improve the dynamic behaviour of the building under an earthquake loading case, the SMA wire-based isolators are implemented into the building and the characteristics of the SMA were determined. Based on the results, it was demonstrated that, with proper damping the proposed new SMARB was effective to reduce the seismic response of the building. Later, the SMARB was compared with the conventional lead rubber bearing (LRB) under seismic study by Wilde et al. (2000) and Gur et al. (2014). The numerical studies presented the comparative response evaluation of the isolated buildings under a set of earthquake data. The parametric study was carried out to identify the optimal design characteristics of both SMARB and LRB system. The results indicated that the SMARB was superior with reference to performance over the traditional LRB. The results showed that, the SMARB provided significantly increase in isolation efficiency, indicating considerable reductions of peak and residual displacement of the bearings compared to the application of elastomeric bearings, such as LRB.

Shinozuka et al. (2015) studied the response of shear building isolated with SMA-based lead rubber bearing (SMA-LRB) through nonlinear random seismic analysis. To evaluate the optimal performance of the device, two design variables are considered such as the strength of the SMA and the yield strength of the LRB. The numerical result indicated that a base isolation system designed with the set of optimal properties of

SMA and LRB was essential to ensure superior performance, by minimizing isolation displacement and increase the isolation efficiency. The parametric study illustrated that the optimal design of isolation, improved the robustness of the isolation system under different earthquake loading and the possible variation in the ranges of the periods of the system.

Qian et al. (2016) proposed the innovative superelastic SMA friction damper (SSMAFD), to reduce the response of structures during an earthquake. The SSMAFD includes a combination of pre-tensioned superelastic SMA wires and friction components. The SMA wire and integrated friction damper were evaluated to contribute to the recentering and energy dissipation capacity. To check the performance of the proposed device, experiments were carried out with a quart scale building under different earthquake records. The structural models with and without SSMAFD were analysed under various earthquake loadings to evaluate the dynamic behaviour of the structure. It is observed from the results that, new device SSMAFD reduced the dynamic response of building subjected to strong earthquake events and demonstrated superior energy dissipation capability with remarkable re-centering ability.

Ghodke and Jangid (2017) proposed a new device, which is a combination of SMA and elastomeric rubber bearing (SMARB) to reduce the structural response of building with base isolation under seismic event. The effect of the isolation time period, the strength of SMA and austenite stiffness on the building response was determined. The results show that, SMA-based isolation devices with the higher modes of base-isolated structures with large austenite stiffness excited with higher acceleration related to higher frequencies were transmitted to superstructures, but the austenite stiffness of SMA did not considerably affect the base displacement and base shear of structures.

2.6 Summary

Based on the literature survey, proposals for newer devices are only available with their component testing and testing along with structures. Analytical methods are restricted to the specific device proposed by the previous study. Most of the proposed methods

are suitable only for small-scale systems and applications in civil engineering. The present research study aims to evaluate the effectiveness of passive damper and to upgrade the strength and improve the seismic performance of building with passive dampers subjected to earthquake excitation. Previous researchers have mentioned the experimental procedure of the frame systems equipped with a variety of passive devices, but FEM-based numerical studies on the combination of passive systems are not yet completely explored. The research contributions have direct relevance to the available methods of XPD and SMAD. A review about the influence of the damping effect on RC frame building subjected to earthquake excitation is presented. Based on these drawbacks considering different types of passive energy, installing dissipating devices-based dampers in buildings are the main aim of the present study.

Table 2.1 Summary of Literature Review

Reference	Description	Method used	Type of analysis
Whittekar et al. (1991)	Conducted experiments on steel plate energy dissipation devices	Experimental	Dynamic loading
Satishkumar et al. (2003)	Proposed passive yielding damper or metallic damper for the reduction of large seismic deformation in building	Experimental and analytical	Dynamic loading
Curedelli and Riera (2004)	Proposed new metallic damper to understand the effectiveness of damper in building	Experimental	Dynamic loading
Bakre et al. (2006)	Proposed XPD for piping system	Analytical	Time history analysis
Parulekar et al. (2009)	Proposed XPD for building system	Experimental	Time history analysis
Pujari and Bakre (2011)	Proposed XPD at different location building system	Analytical	Time history analysis and simulation by SAP2000 software
Grasser and Cozzarelli (1991)	Proposed one dimensional stress induced model to understand large deformation in SMA	Experimental	Dynamic loading
Desroches et al. (2004)	Studied the behaviour of SMA wires and bars with different diameter	Experimental	Tests on SMA wire and bar
Dolce et al. (2000)	Proposed SMA device for building system	Experimental	Dynamic loading
Wilson and Wesolowsky (2013)	Studied the performance of building with isolators and SMAs	Experimental	Earthquake loading
Ghodke and Jangid (2017)	Proposed new device combination of SMA and elastomeric rubber bearing	Experimental	Earthquake loading

2.7 Problem Identification

To develop seismic design incorporating latest seismic technology with control devices to withstand building from earthquake is one of the major research area. The past research study deals with the proposal for new devices, their component testing and testing along with structures. The explanation of the analytical method is restricted to the specific device proposed by the researchers. Most of the proposed methods are suitable only for small-scale systems and applications in civil engineering field. The study on the finite element based numerical methods of the building with damper under seismic excitation has not been carried out extensively. Also, a combination of two dampers and design parameters of these devices for their inclusion in the systems is required. The integrated computer code is also required for dynamic analysis of a building system equipped with passive devices. The present study aims to determine the effectiveness of passive dampers considered to improve the design and performance of structures during an earthquake. Based on previous research studies, experimental procedure of the building frame systems equipped with a variety of passive devices were explained but, studies on combinations of passive systems are not completely explored. Therefore, consideration of two different types of passive energy dissipating device-based dampers is considered in the present study.

CHAPTER 3

MATHEMATICAL FORMULATION

3.1 General

The cyclic deformation of X-plate damper (XPD) and shape memory alloy damper (SMAD) acts as nonlinear when accompanied by the continuous and repeated application of cyclic load on yielding steel material and SMA wires leads to changes in stiffness of material. The main property of both XPD and SMAD, in the cyclic deformation tests of metal plates and wires are subjected to loading, these plates and wires consume a substantial amount of the structural vibration energy in the form of hysteretic mechanism. In this chapter, the mathematical formulation of XPD and SMAD and their initial properties are discussed in detail.

3.2 Mechanism of X-Plate Damper (XPD)

XPD is made up of steel and it can sustain many cycles from stable to yielding deformation. It is a hysteretic device due to its energy dissipation capacity. XPD maintains a constant strain over total height of the device, thus ensuring that yielding occurs uniformly throughout the height of the damper (Figure 3.1). During the last few years, XPDs are being developed as good energy dissipation devices in seismic response control of the piping system, structures and in the nuclear industry. The experiments were conducted on different possible size and shape of the XPD by a few researchers in the past. The results illustrated that, XPDs are having high-quality absorbing and dissipation of vibration energy subjected to earthquake. The properties of the X-shaped plate were found that using the beam theory (Satishkumar et al. 2003).

For the last few years, researchers are experiments are conducted by BARC (Mumbai) and SERC (Madras) on different possible configurations of EPD and also to develop EPDs as an extensive tool for seismic response control of piping in the nuclear industry and buildings. EPDs resulted in promising results by absorbing the vibration energy

during earthquakes. The design and test characteristics of EPDs have been explained in the following sections.

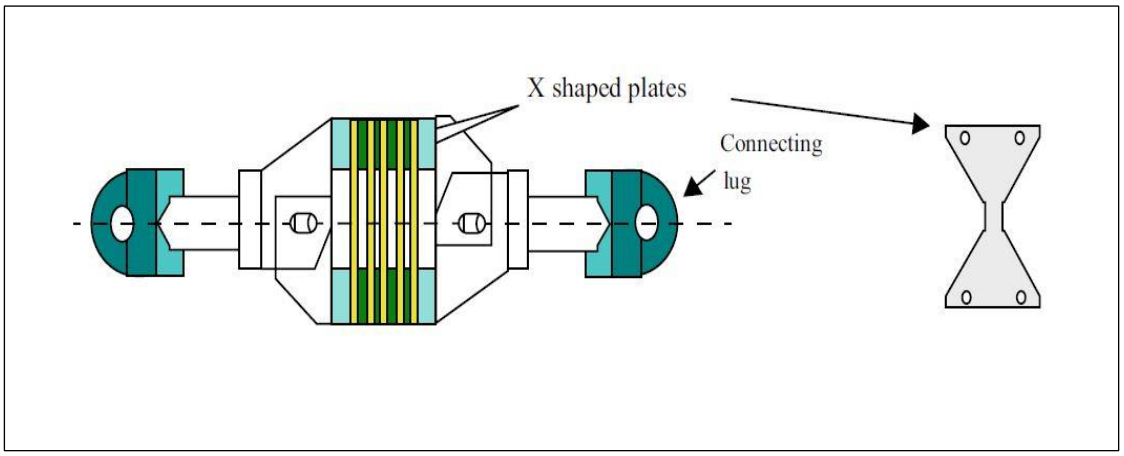

Figure 3.1 Schematic diagram of X-plate damper (Satishkumar et al. 2003)

3.2.1 Characteristics of X-Plate

The main features of the X-plate are force and displacement are obtained using analytical formulations and via conducting static and cyclic tests on X-plate on various properties as size, shape and thickness. The force-displacement curve for an X-plate was obtained using the beam theory as shown in Figure 3.2. The expressions are derived for three cases as follows (Equation 3.1, 3.2, 3.3 and 3.4),

Considering the top portion of the X-plate i.e. triangular plate with bending stress in X-plate is elastic. Thus, the top of two triangular plates made the total X shaped plate.

$$F = \frac{Ebt^3 d}{6a^3} \tag{3.1}$$

For X-plate, the stiffness can be expressed as,

$$K = \frac{Ebt^3}{12a^3} \tag{3.2}$$

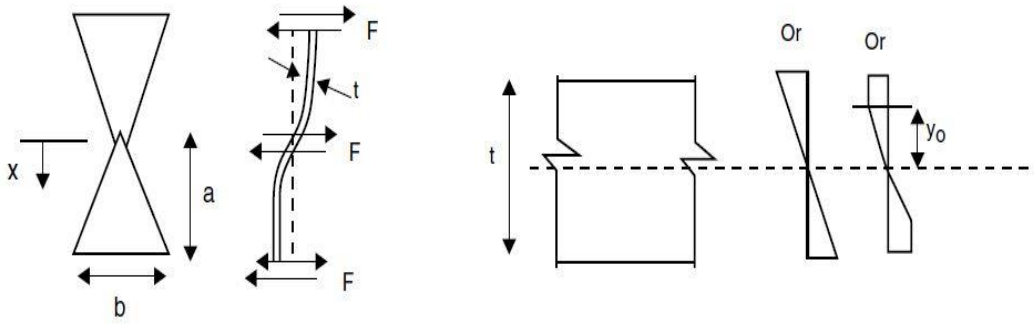

Figure 3.2 Characteristics of X-plate damper (Parulekar, 2003)

In X-plate the bending stress just reaching yield stress for a triangular plate,

$$F_y = \frac{\sigma_y \, bt^2}{6a} \tag{3.3}$$

The yield displacement of X-plate,

$$d_y = \frac{\sigma_y \, a^2}{Et} \tag{3.4}$$

Where,

a = height of the triangular plate

b = width of the triangular plate

d = displacement

E = modulus of elasticity

K = stiffness of the plate

t = thickness of the plate

Using the above equations, the properties of 3mm and 6mm thick carbon steel material X-plate properties are obtained. Values of E= 2.1 x 10^5MPa, and σ_y= 220MPa have been used for analysis.

3.3 Mechanism of Shape Memory Alloy Damper (SMAD)

The analysis of the constitutive models of SMAs is complex. The simple constitutive model of SMA for dynamic analysis of structures is investigated. The constitutive model was adopted in the present research study developed by previous researchers to provide a multilinear stress-strain relationship. The phase transformation of SMA during the process of changing from austenite to martensite or vice versa is called reversible transformation characteristics. The material parameters of SMA models are specified by austenitic elastic modulus E_A, the starting and final stresses and the transformation strain ε_l and the direct and inverse transformation. To obtain the data required to assess the dynamic behavior of SMA model capacity, experimental tests were conducted.

3.3.1 Pseudoelastic property of SMA wire

SMA wire subjected to stress induced mechanical loading results in change in the phase transformation from austenitic state to martensitic state. During this phase transformation process, by the removal of external load, the SMAs come to its initial shape. This process is known as pseudoelastic effect. Figure.3.3 shows pseudoelastic stress-strain diagram of SMA wire. In the uniaxial test, the stress strain behaviour of austenitic SMA wire characteristic are measured.

During loading path of SMA wire (o-a-b-c), the stress level of the wire reaches to austenite start stress state σ_{Ms}. At constant stress levels, the austenite SMA wire transforms to martensite stress state and vice versa. This will continue until all the austenite has been transferred to matrensite state. During allowing of stress, martensite state unloading (c-d) elastically down to austenite start to stress, $\sigma_{As,}$ at constant stress level the austenite transform back (d-e'). After completion of this transformation process, final elastic unloading (e′-o′) of the austenite phase takes place. This procedure is known as superelastic effect of pseudoelastic since the behaviour is nonlinear, there is no permanent deformation. However, at the end of unloading of wire to zero load case there is some finite residual deformation of the wire retained. When the austenitic

Ni-Ti SMA wire subjected to cyclic load experimentally, some amount of residual martensite is retained as observed by Miyazaki et.al (1986). To reach the residual strain at a value of 0.4% to 0.5%, an increase in number of cycles progressively increases the residual martensite strain about 50 cycles. At the grain boundaries, the local stress is created which locally induces martensite and retains it. The apparent modulus of austenite was assessed while loading and unloading of SMA wire and found measured magnitude of deformation by Liu and Xiang (1998). The e′o′ is the slope during unloading, while unloading the apparent modulus of elasticity of austenite was found to be 80% that loading of wire with maximum phase transformation strain. At the end of loading 50 cycles the residual martensite is retained (oo′) is as shown in Figure.3.3.

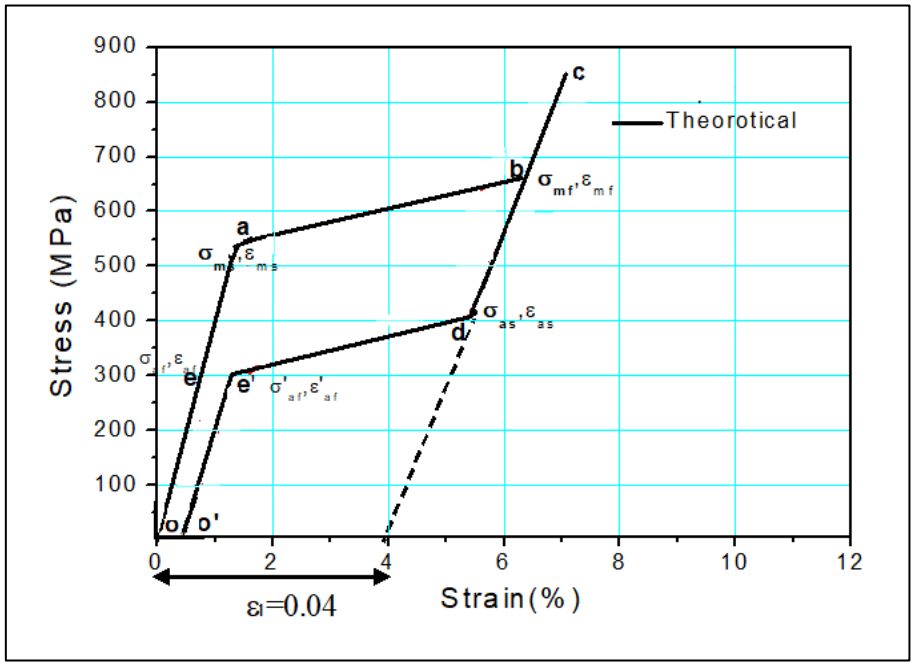

Figure 3.3 Pseudoelastic stress-strain diagram of SMA wire (Motahari and Ghassemieh 2007)

3.3.2 Thermomechanical model of SMA

The existing SMA thermomechanical model was considered by Motahari and Ghassemieh (2007), during cyclic behaviour of SMA wire. In the uniaxial experiment tests of SMA wire, while unloading the austenite SMA wire, the residual deformation is and the apparent modulus of elasticity was observed. Further, to facilitate the application of SMA wire in civil engineering field an effective and simplified constitutive model needs to be designed. Earlier researchers proposed few models of mechanical behavior of SMA wire (Tanaka et al. 1986, Grasser and Cozzarelli 1991, Liang and Rogers 1992, Brinson 1993, Boyd and Lagoudas 1996). Among these models, the Boyd and Lagoudas (1996) model is more simplified and suitable model is for practical use in engineering field. The multilinear stress-strain thermomechanical model of SMA is considered in the present study as investigated by Boyd and Lagoudas (1996).

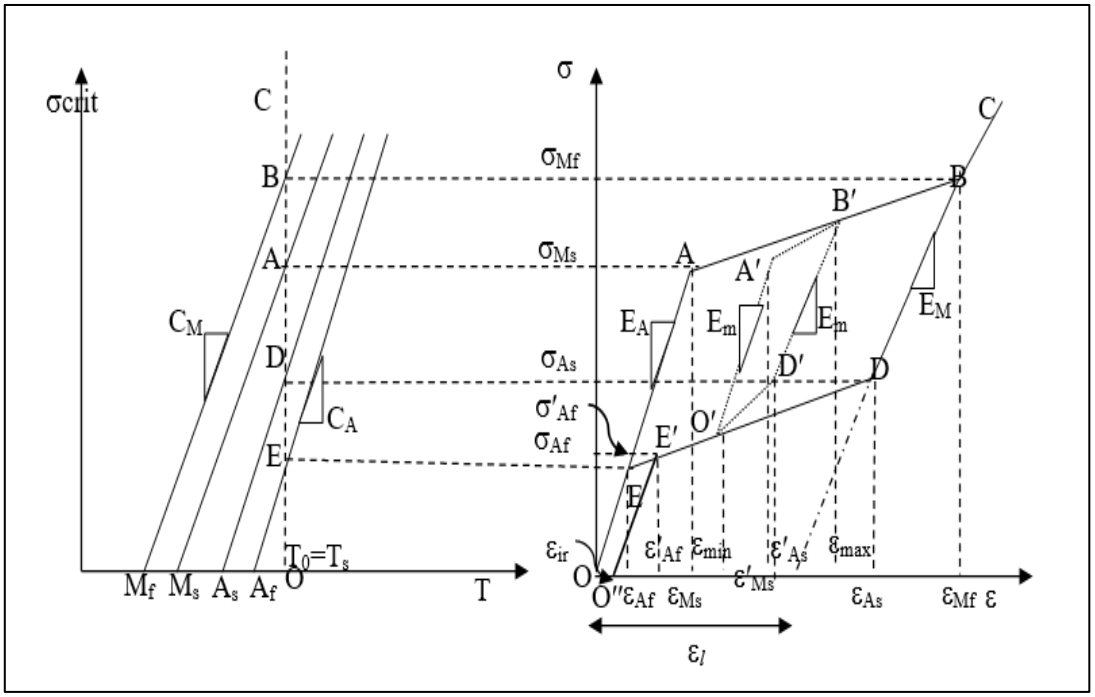

Figure 3.4 The multilinear stress strain diagram (Motahari and Ghassemieh 2007)

In the present work, the thermomechanical model of Parulekar et al. (2012) is considered, in which the proposed modified model by Motahari and Ghassemieh (2007) proposed the residual martensite strain hardening of SMA wire and the decrease of modulus of elasticity of the austenite is taken in this study. In this model during cyclic phase transformation of SMA wire, due to incomplete phase transformation of cycles, the residual cyclic loading effect is produced and sub looping behavior of SMAs is observed. Using the constitutive relation (Equation 3.5), the uniaxial thermomechanical behavior of SMAs can be described (Parulekar et al. 2014).

$$\sigma = E(\xi)\varepsilon - \alpha(\xi)E(\xi)(T - T_s) - E(\xi)\xi\varepsilon_l \tag{3.5}$$

The evolution equation for SMAs is the relationship between martensite fraction ξ ha exponential and polynomial of various thermomechanical models of SMAs (Tanaka 1986 and Brinson 1993). The evolution equation imposed the linear relationship between stress and strains model used in the present study. This model is modified when the pseudoelastic wire is unloaded in the path of the stress-strain relation path and consider the residual martensite strain of 0.45% is considered.

The isothermal process ($T=T_s$) for super-elastic behavior is considered and using Equation 3.5, the following equation (Equation 3.6) was developed.

$$\sigma = E(\xi)\varepsilon - E(\xi)\xi\varepsilon_l \tag{3.6}$$

The Young's moduli of austenite state E_A and martensite state E_M respectively. The Equation (3.6) can be written as by considering the polycrystalline SMAs in terms of Equation (3.7) and Equation (3.8)

$$E(\xi) = E_A + (E_M - E_A)\xi \tag{3.7}$$

$$\sigma = E(\xi)\varepsilon - E(\xi)\xi\varepsilon_l = a\varepsilon + b \tag{3.8}$$

The model is pass through by achieve the model to finish the critical stresses and strains 'a' and 'b' are obtained.

In the present study, the uniaxial experimental tests on SMA wires was conducted at room temperature T_s=35^{0}C and transformation temperatures are M_f=80^{o}C, M_s=-60^{o}C, A_s=-25^{o}C and A_f= -8^{o}C were considered. The stress-strain relationship of the simplified model of SMA damper device considering the effect of residual martensite strain is as shown in Figure 3.5. Using the uniaxial test results of SMA wire and the relation between stress-strain curve of wire the critical stresses (σ_{Ms}, σ_{Mf}, σ_{As} and σ_{Af}) and strains (ε_{Ms}, ε_{Mf}, ε_{As} and ε_{Af}) are obtained as shown in Figure 3.4 and are σ_{Ms}= 551MPa, σ_{Mf}=667MPa, σ_{As}=402MPa and σ_{Af}=288.1MPa and the critical strains are ε_{Ms}=0.013, ε_{Mf} =0.064, ε_{As} =0.054 and ε_{Af}=0.0068 and also the maximum value of residual martensite strain, ε_{ir} = 0.0045, σ'_{Af}=299MPa, ε'_{Af}=0.0113, Young's moduli of austenite and martensite are E_A= 42308MPa, E_M =28571MPa, and the total phase strain value, ε_l =0.04 respectively.

Liu and Xiang (1998) studied that, while unloading and reloading process of NiTi SMA wire, the Modulus of elasticity austenite E_A, NiTi wire for unloading was measured and it was found that the 15-20% lower than that for loading case. When the apparent elastic deformation of austenite NiTi wire specimen and the contribution of a second deformation mechanism occurs, this deformation may be either the stress induced martensitic transformation or martensite reorientation. Therefore, the modulus of elasticity while unloading is 35055 respectively, and the σ'_{Af} and ε'_{Af} are 303.44 MPa and 0.0132 respectively.

The pseudo-elastic NiTi alloys, multi-linear stress strain diagram with loading path is as shown in Figure.3.4. For the pseudo-elastic NiTi alloys the transformation constants C_A is 6.7MPa and C_M is 5.8MPa are obtained and it can be illustrated in the form of Equation 3.9 to Equation 3.12 (Lagoudas (1994). The Figure 3.4 shows that, at fully loading transformation state of SMA wire changes from in the major loading path O-A-B-C-B-D-E-O to the minor loading path 1-2-3-4-1 under incomplete transformation state. In stress temperature phase diagram, the basic parameters include the slopes of forward phase transformation C_M and reverse phase transformation state C_A and the four zero stress transformation temperatures are M_s martensite starting temperature, M_f

the martensite finishing temperature, A_s the austenite starting temperature and A_f austenite finishing temperature corresponding E_A the austenite elastic modulus and E_M martensite elastic modulus, and ε_l the maximum transformation strain and the equation are as follows

Path O-A and E-O, loading elastically completely austenitic state,

$$\sigma = E_A \varepsilon \tag{3.9}$$

Path A-B, loading forward transformation

$$\sigma = \sigma_{Ms} + \frac{\sigma_{Mf} - \sigma_{Ms}}{\varepsilon_{Mf} - \varepsilon_{Ms}} (\varepsilon - \varepsilon_{Ms}) \tag{3.10}$$

Path B-C and C-D, unloading elastically completely martensite state

$$\sigma = \sigma_{Mf} + E_M (\varepsilon - \varepsilon_{Mf}) \tag{3.11}$$

Path D-E$'$, unloading reverse transformation,

$$\sigma = \sigma_{As} + \frac{\sigma'_{Af} - \sigma_{As}}{\varepsilon'_{Af} - \varepsilon_{As}} (\varepsilon - \varepsilon_{As}) \tag{3.12}$$

Unloading in elastic austenitic state with residual martensite strain is in terms of Equation (3.13) for $\varepsilon < \varepsilon'_{Af}$ (i.e., 0.0132),

Path E′O″

$$\sigma = \frac{\sigma'_{Af}}{\varepsilon'_{Af} - \varepsilon_{ir}} (\varepsilon - \varepsilon_{ir}) \tag{3.13}$$

σ'_{af} and ε'_{Af} are the stress and strain corresponding to austenite finish states, considering the residual strain ε_{ir}. For complete martensite transformation the maximum value of strain $\varepsilon_{ir\,max}$ strain is limited to 0.45%. The residual martensite fraction Z_{ir} depends on an incomplete cycle of martensite transformation residual stress (Lexcellent and Bourbon 1996). The Equation 3.14 to Equation 3.15 (Lexcellent and Bourbon 1996) is shows the maximum residual strain is related to the maximum residual martensite fraction.

$$\varepsilon_{ir} = l_{ir_{max}} \tag{3.14}$$

The total phase strain is ε_l=0.04. For the incomplete phase transformation strain and γ the residual martensite strain will be given by the following equation

$$\varepsilon_{ir} = \frac{\varepsilon_{irmax}}{\varepsilon_l} \tag{3.15}$$

Before the completion of the forward phase transformation or while starting of reloading condition and while unloading the elastic stiffness for both austenite and martensite phases will be different. If L_m and L_a are the compliances of mixture constituents and they have a linear relationship with strain is given by following Equation (3.16)

$$L_m = x\, L_M + (1-x)\, LA \tag{3.16}$$

In which *x* is $\frac{\varepsilon Ms_{max}}{\varepsilon_{Mf}-\varepsilon_{Ms}}$ for unloading and *x* is $\frac{\varepsilon Af_{min}}{\varepsilon_{As}-\varepsilon_{Af}}$ for reloading

Before unloading or reloading state ε_{max} and ε_{min} are maximum and minimum strains as shown in Figure. 3.4. The elastic stiffness is given by Equation (3.17) (Parulekar et al. 2014)

$$E_m = \frac{E_M E_A}{x(E_A-E_M)+E_M} \tag{3.17}$$

The critical austenite strain values will be found from Equation (3.18) as follows

$$\varepsilon'_{As} = \varepsilon \frac{\sigma_{As}-\sigma_{max}}{E_m}_{max} \tag{3.18}$$

The stress-strain relations on the sub-loop paths is Path O′A′-A′B′-B′D′-D′O′ as shown in Figure 3.4. From experimental SMA wire result indicates that the σ_{max} maximum and σ_{min} minimum stresses are obtained corresponding to ε_{max} maximum and ε_{min} minimum strains are found and it is given by Equation (3.19) (Parulekar et al. 2014) it is as follows

Path O-A and E-O, loading elastically completely austenitic state

$$\sigma = E_A \varepsilon \tag{3.19}$$

Where,

σ = stress

ε = strain

T= temperature

T_s = start temperature

σ_{Ms} = Martensite start stress

σ_{Mf} = Martensite finish stress

σ_{As} = Austenite start stress

σ_{Af} = Austenite finish stress

ε_{Ms} = Martensite start stress

ε_{Mf} = Martensite finish strain

ε_{As} = Austenite start strain

ε_{Af} = Austenite finish strain

E = effective Young's modulus

α = effective coefficient of thermal expansion

ε_l = maximum phase strain

ξ = volume fraction of the martensite phase

3.3.3 Configuration of SMA damper

The SMA device was designed based on the energy dissipation properties of Ni-Ti wires and to evaluate the mechanical properties of the SMA wire. The device is made up of austenitic wires having recentering and energy dissipating property and consists of two concentric mutually movable pipes. SMA wires having length of 120mm and inner pipe consists of three studs and outer pipe consists of six studs are attached at an equidistance of 120mm. The length of the wire can be increased to get a good stroke length of the damper. During tensile tests, to prevent the slipping or sliding of the wires, they are fixed with collets to the studs. Thus, total 6 number of wires each with 1.2mm diameter connected to damper studs. At room temperature 35^0C, the tension and then compression sinusoidal loading testing of damper was conducted. The SMA wire tests are carried out and it was observed that wires can dissipate energy of up to 8% of strain. Thus, it is recommended to use as energy dissipators. Based on test results of SMA

wire, the SMA damper can be tested. The damper consists of total six number of SMA wire three on tension side and three are slack. During testing the one end of the damper is connected to actuator and other end is fixed and while in loading condition the three wires of damper are in tension and other three wires are on slack side. The experimental tests were carried out at quasistatic loading condition of frequency 0.01Hz to predominant loading condition of frequency 0.1Hz to 5Hz. At 3Hz one cycle loading rate case it was observed that the stress at austenite start transformation (σ_{as}) path remains the same and at different amplitude of loading rate the unloading paths are different as shown in Figure 3.5. Thus, two types of group of wires can be provided, which will act as energy dissipation system. The three wires on tension side will dissipate earthquake energy and remaining less energy as transmitted to the structural system (Parulekar et al.2014).

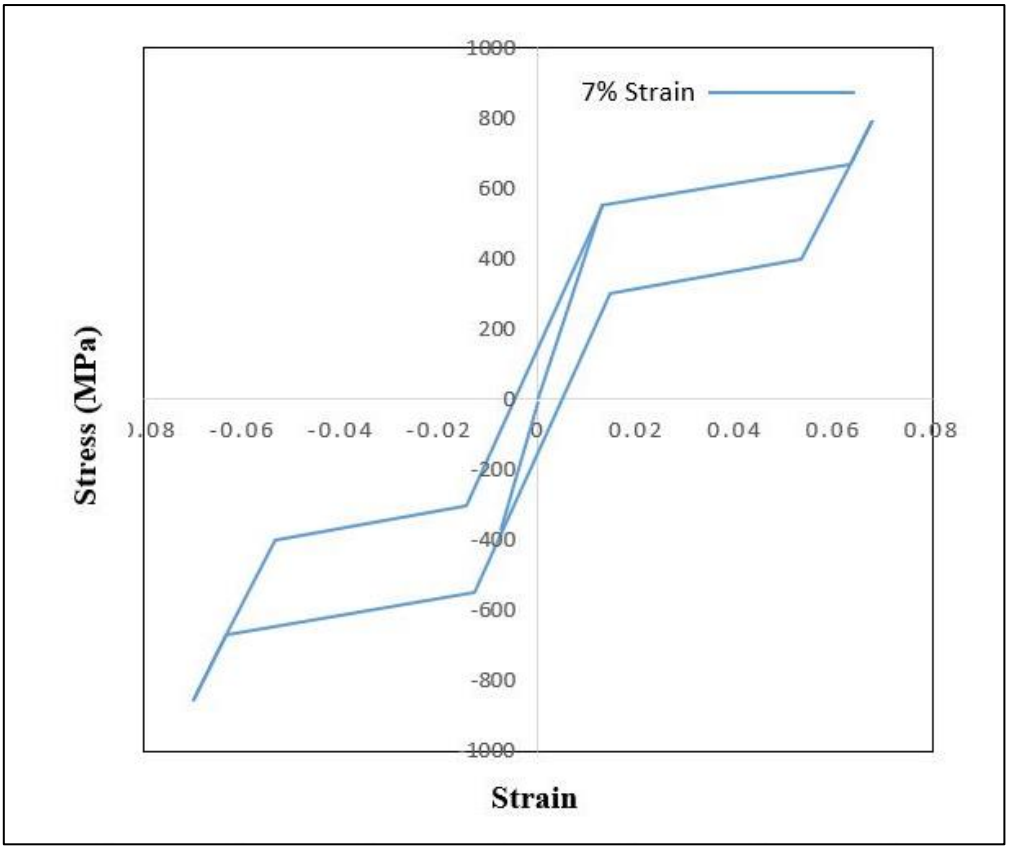

Figure. 3.5 Stress-strain relationship of SMA damper (Parulekar et al. 2014)

CHAPTER 4

NUMERICAL ANALYSIS

4.1 General

This chapter deals with the finite element analysis of building, performed using ANSYS software. To build the finite element model in ANSYS 2016, to run the model efficiently there are several steps to be involved. The models can be generated using quick command line or graphical user interface system (GUI). In the present study, to build the model the GUI has been used. This section describes in detail about the finite element modelling and analysis of controlled and uncontrolled R.C.C structure and the different steps and inputs used to create the finite element model using ANSYS version 16 software.

4.2 Details of the R.C.C Building

The residential building of height of each storey 3m and beam width size of 4m was considered for the parametric study. The RC frames are designed as per Bureau of Indian Standard codes, IS 456-2016, "plain reinforced concrete code of practice", IS 1893-2002 (Part1) criteria for earthquake resistant design of structure", and detailed as per IS 13920-2016 ductile detailing of reinforced concrete structures subjected to seismic forces. The grade of concrete is M25. The experimental test carried out by the Earthquake Engineering and Vibration Research Centre (EVRC) of Central Power Research Institute (CPRI) Bangalore. The shake table size is 3m × 3m and having the payload capacity is 10 tons. Because of shake table size and weight restrictions, the structure had to be scaled down to approximately one third scale of the actual size. The model and plan of 3D RC structure is as shown in Figure 4.1 and Figure 4.2. The construction details of three-dimensional RC structure are tabulated in Table 4.1. The height of each storey is 0.9m and width of each bay is 1.2m and the size beams and columns of 3D prototype RC structure is 75mm x100mm, 50mm thick slab as shown in shown in Figure 4.3.

Figure 4.1 Model of 3D RC structure ((Chetan et al. 2009 and CPRI Bangalore)

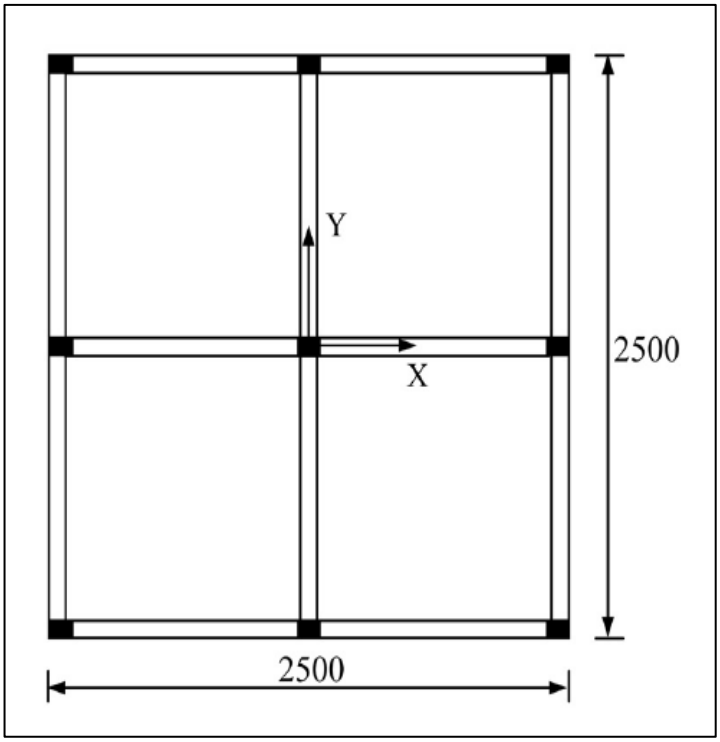

Figure 4.2 Plan of RC structure (Chetan et al. 2009)

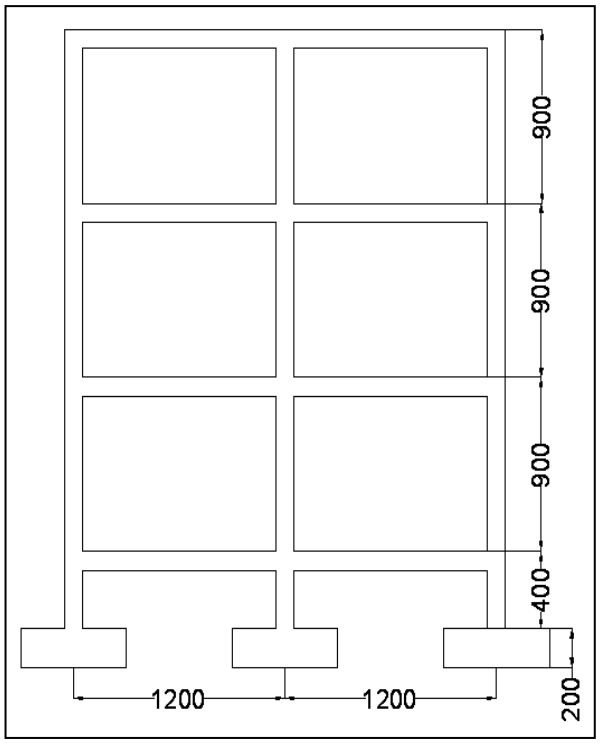

Figure 4.3 Elevation of RC structure (Chetan et al. 2009)

Table 4.1 Details of RC structure

Description	3D R.C.C structure
No. of storeys	3
No. of bays	2
Storey Height	0.9m
Bay width	1.2m
Beam and Column	75mm x100mm
Slab	50m thick

4.3 ANSYS Modelling

The finite element analysis includes the modelling of a reinforced concrete building, with the dimensions and section properties matching to the experimental data. Ansys provides a high definition graphics capability that can be used to display results of the analysis. It can accurately represent complex geometry, include dissimilar properties,

captures local effects and can represent the total solution easily. The study includes modelling of R.C.C building using ANSYS 16 finite element software. The various steps involved in modelling is discussed in the following sections.

Steps for modelling:

Finite element modelling is divided into three main stages

i. Pre-processing
   a) Building a FEM model
   b) Geometry creation
   c) Mesh generation
   d) Application of boundary and loading conditions
ii. Submitting the model to ANSYS
iii. Solver
iv. Post-processing
   a) Checking and evaluating results
   b) Presentation of results

The first step includes defining element type, key points, lines and areas of the model and next assigning material properties, proper sections, meshing the lines and areas of the model. In second step, loads and boundary conditions are applied and the problem is solved. The last step includes listing the results, plot the results, etc.

The finite element analysis of any model specimen requires the meshing of the specimen or model created. In Ansys software the mesh can be generated in two methods are solid modelling method and the direct generation method. In the solid modelling method, the user defines the size, shape and boundary values of the object, to provide and control the element system and mesh sizes and software generates key point, node, meshes and element automatically. But, in case of direct generation method, the user defines the whole geometries, elements, meshes and nodes of the whole object. Before meshing is done, mesh attributes must be properly selected to assign the material properties. Material number, real constants, material properties corresponding to each part of the model must be assigned. The material properties assigned to beam and mass element.

To get the accurate solution of the model, displacement boundary conditions constraints are applied. To ensure that the model acts the same way as the R.C.C building, where the supports and loading exists boundary condition constraints to be applied if required at the point of symmetry. The support conditions are modeled in such a way that a fixed end was created. All the nodes on the bottom side of the column were given constraints in the UX, UY and UZ directions.

The imposed load and total dead load to 25% of the imposed load as per the code provisions. Dead loads are given by assigning density to the models as material definitions. The load is applied in the pressure on the nodes of the model.

a) Analysis method
b) Nonlinear solution

Nonlinear structural behavior arises from a number of causes, which can be grouped into this principal category

a) Changing status
b) Geometric nonlinearity
c) Material nonlinearity

The nonlinear structural behavior, which includes one of the common properties is material nonlinearity. The structure influences many factors such as material nonlinearity, temperature effect and loading conditions. To solve nonlinear problems in Ansys software Newton Raphson method is employed. In this method, the load can be applied over the increments and load is subdivided into a sequence of load increments.

4.4 Modelling of R.C.C Structure

The finite element method is an efficient method to analyze the complex structures. The 3D integrated finite element model of R.C.C building is created using ANSYS 16 software package to obtain the structural parameters and to calculate the efficiency of vibration reduction in the building with damper subjected to earthquake ground motion

and the flow chart of computational model is as shown in Figure 12. The procedure followed to analyse in ANSYS software is discussed in detail below.

- **Element type**

The members of the building beam and columns are modelled with beam element is as shown in Figure 4.4 with six degrees of freedom per node for space structures. The slab of the building is modelled using shell element is as shown in Figure 4.5 for bending and membrane capabilities, having six degrees of freedom at each node and the input parameters are the thickness of the slab. A precise mesh size was achieved by analysing building design model, modifying mesh, re-analysing and repeating the cycle till convergence was achieved.

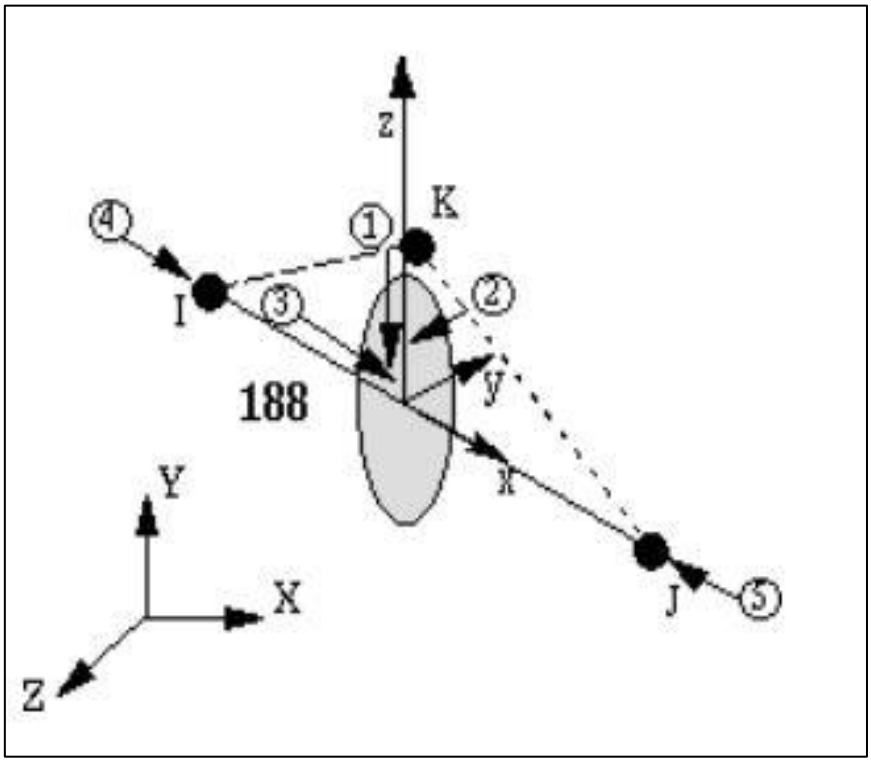

Figure 4.4 3D linear beam element (ANSYS 16)

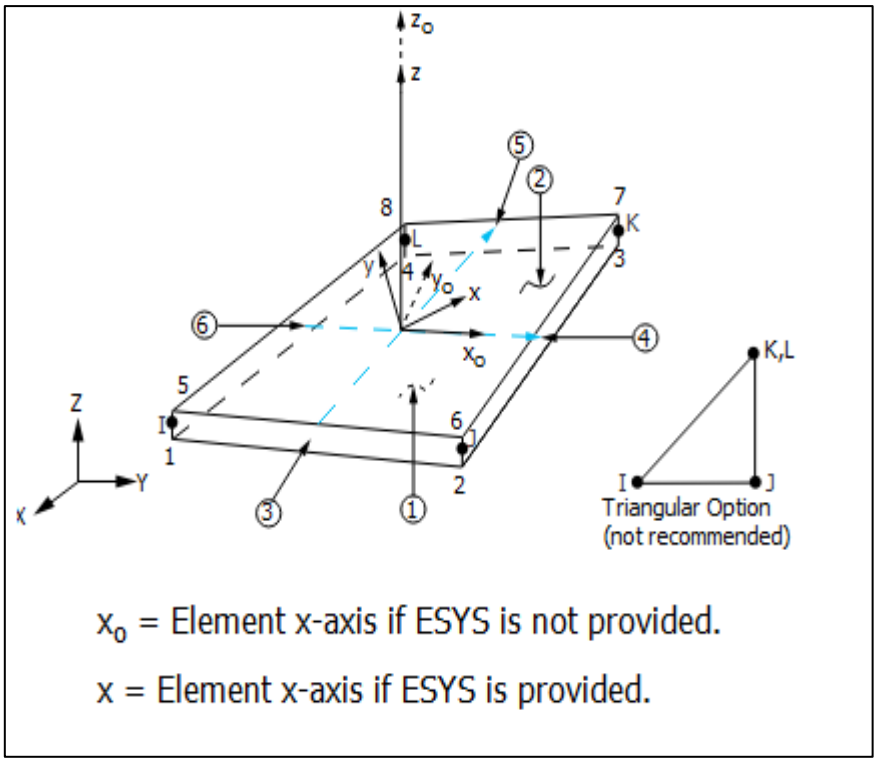

Figure 4.5 3D shell element (ANSYS16)

Material Property

The material properties of building are defined and assigned to each element as tabulated in Table 4.2. The beam and column cross sections were modelled. In that element formulation, the input parameters are moment of inertia along X and Y and polar moment of inertia J. Mass of the building is assumed to be distributed on the floor area of the building.

Boundary condition

The finite element model of R.C.C building is created and fixed boundary conditions are applied at the base of the building.

The two main non-linear analysis are: modal analysis and time history analysis. These are discussed in below.

- **Modal analysis**

Modal analysis was initially performed with application of self-weight of the building model to generate a fundamental natural period of the models in the present study. It is done using Block Lancozs extraction method which uses sparse matrix solver. The plan and 3D model of building is as shown in Figure 4.4.

- **Time history analysis**

Time history displays the earthquake induced motion as a function of time. The simulated motion is derived from existing or artificially generated earthquake records. In time history analysis method, the loading and the response history are determined at successive time increment. At every step, analysis starts from initial condition and the response is evaluated from the existing of the beginning step. In linear time history, the structure behaviour is assumed to be remain linear throughout the analysis. In nonlinear analysis the behaviour of the structure is considered based on the structural properties. Thus, to evaluate the nonlinear response of the structure this method is very effective. In nonlinear dynamic analysis of object created or specimen model is analysed using the Newmark step by step integration method which is very useful technique. In this analysis of the dynamic response of a structure or any object created subjected to specified ground motion data with respect to time. The input given as a ground acceleration time history data is applied uniformly at all the points of the base of the structure. The input time history consisting of scaled natural accelerograms records is employed for the dynamic analysis of the present study. The time history of the Elcentro earthquake ground motion with 0.1g PGA value is considered.

Ground motion records of Elcentro earthquake: The main earthquake record is in 1940 at Elcentro Imperial Valley. But in the present study, Elcentro earthquake data is used because it is having highest magnitude of 9.2 that has ever been recorded. This earthquake experienced resulted in very high amount of damages to the buildings.

In Figure 4.6, the input data Elcentro earthquake, the time against ground acceleration time history is plotted.

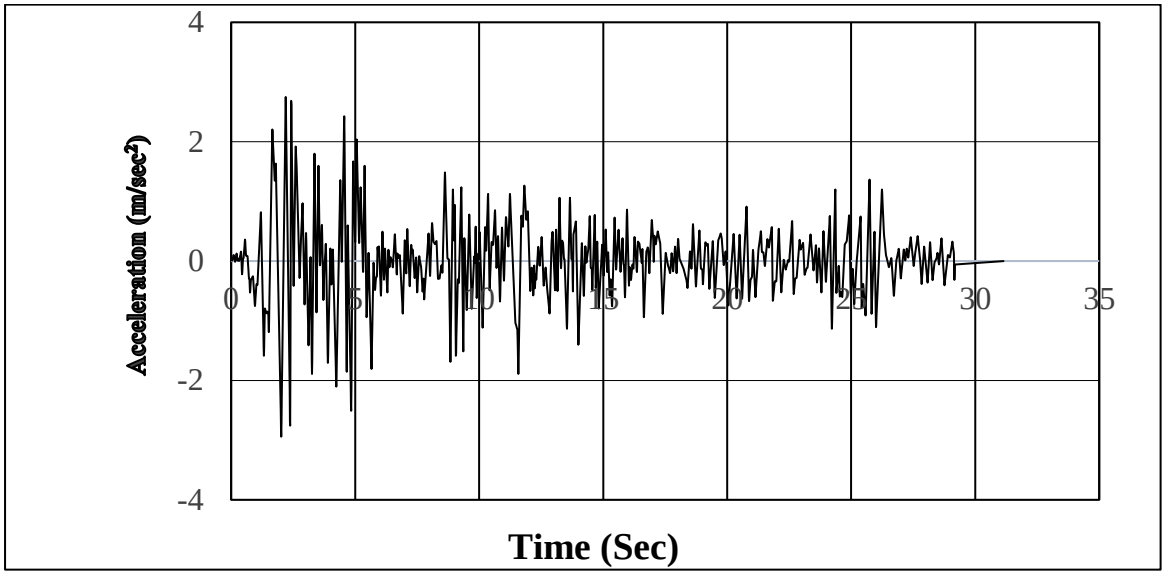

Figure 4.6 Input ground acceleration record for El Centro earthquake

Structural system is often idealized as a discrete model. The damping coefficient of 5% critical damping was applied to the model to facilitate the damping effects. The full transient dynamic analysis is carried out using Newmark Beta method on the building model. Analysis of conventional building with fixed base R.C.C building and with damper is carried out subjected to real time data of El Centro earthquake with values of base acceleration of 0.1g PGA and time interval of 0.02sec. The damper is modelled using Combin40 element as shown in Figure 4.7. In dynamic analysis of basic damper system, the combin40 element was used, because of large number of degrees of freedom in the beam element. Combin40 element is combination of spring constants K1 and K2 and F sliding force as a slider, damper in parallel coupled to a gap size GAP in series. The mass M can be applied at node I and node J or it is distributed equally and C is damping coefficient. When the load decreases smaller than the sliding force FSLIDE the elastic stiffness is (K1+K2) and if sliding force increases, the yielding stiffness changes to K2.

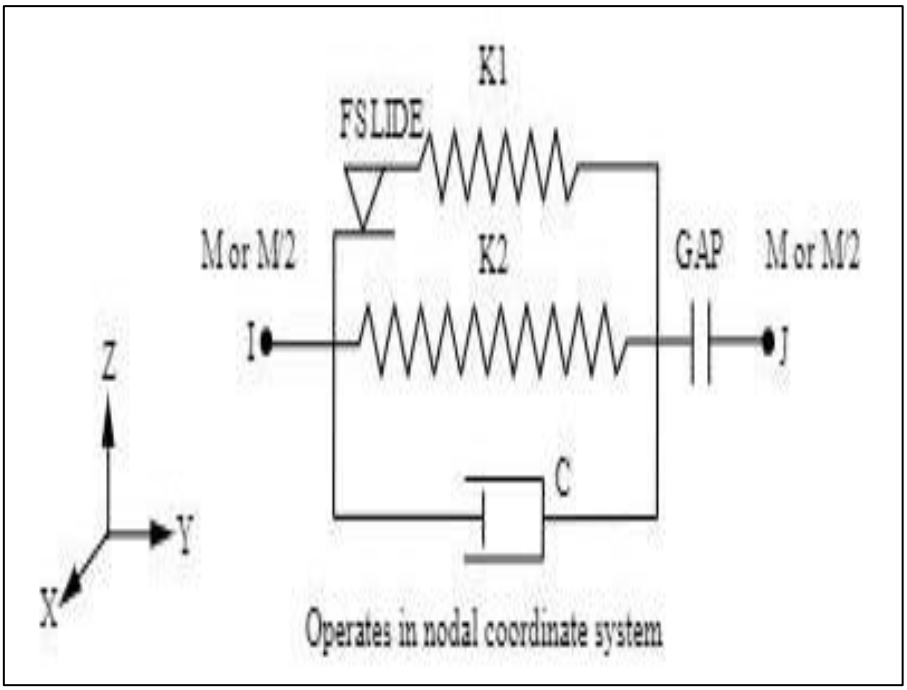

Figure 4.7 Configuration of COMBIN40 element (ANSYS16)

Table 4.2 Material properties of RC structure

Material	Concrete
Modulus of Elasticity E_S (MPa)	2.871×10^5
Poisson's ratio (μ)	0.22
Unit weight (kN/m^3)	24

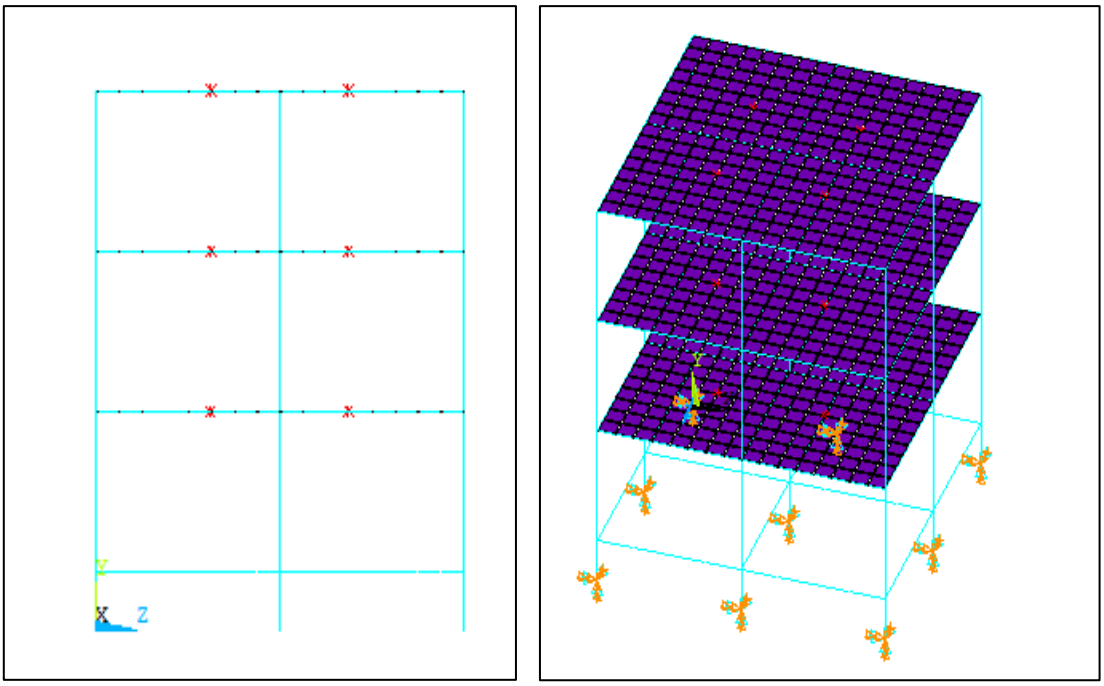

Figure 4.8 Plan and elevation of FEM model of 3D RC structure

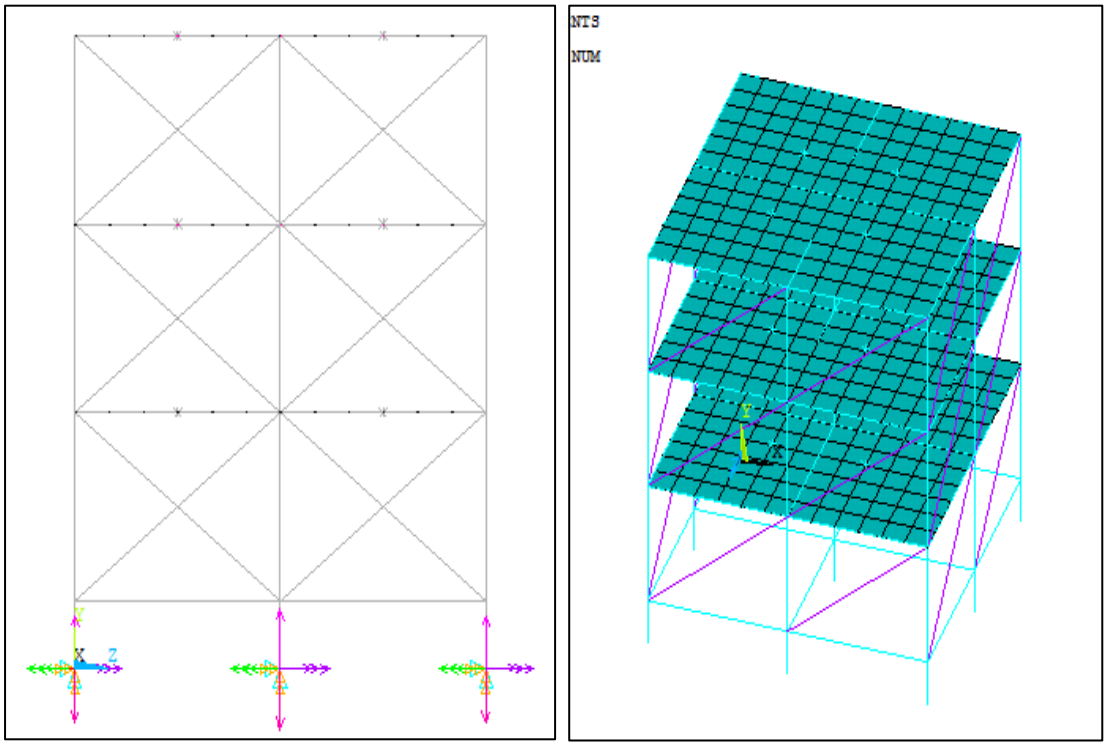

Figure 4.9 FEM model of 3D RC structure with damper

4.5 Modelling of XPD

The R.C.C structure considered in the present study is made up of beam element and column and fixed at the base as explained in previous section 4.4. and Figure 4.8 and Figure 4.9 show the FE model of the R.C.C structure building with and without damper. The following assumptions were made for seismic analysis of an R.C.C structure building with XPD.

i. Installation of XPD damper in building should be determined first. The two diagonal fixed points of each XPD damper should be determined mainly. In the present study, an XPD damper is placed diagonally between two points of each storey of the building.
ii. During simulation of XPD in building, whereas building system remains linear and only XPDs behave as nonlinear.
iii. The force-displacement behavior of the XPD is considered as hysteretic, based on the nonlinear model. The non-linearity was assumed to follow the stress-strain values after the yield point were input from stress-stain characteristic of the material. The force and displacement values thus obtained have been plotted at different displacement.
iv. The bilinear elasto plastic material model where the initial elastic stress strain curve, followed by a curve with plastic deformation is considered. The size and material properties of the single XPD is given in Table 4.3. To simulate the mechanical properties of the metal, the equivalent stiffness method is used. The analysis is carried out for three cases, one with plate size having a=b=40mm and a=b=60mm with 3mm and 6mm thick plate. The material model of XPD is simulated using bilinear model available in ANSYS material model library. The time history analysis of the building with XPD is carried out under earthquake loading excitation applied in X-direction. The lateral displacement and accelerations of the building are evaluated.

Table 4.3 Properties of single X-plate (Parulekar et al. 2003)

Parameters	value	Units
Modulus of Elasticity (E)	2.1×10^5	MPa
Yield Stress (σ_y)	220	MPa
Thickness of the plate (t)	3,6	mm
Breadth of a triangular portion (b)	40,60	mm
Height of a triangular portion (a)	40,60	mm

4.6 Modelling of SMA

To understand the behaviour of 3D R.C.C structure equipped with SMA wire dampers numerical analysis is carried out and presented in this section. The concept of SMA wire is discussed in Chapter 3, to make use of SMA damper in the building and to decrease the response of building under high seismic event.

The two different SMA damper consists of 0.4mm diameter and 1.2mm diameter SMA wire. When structure with the SMA damper is vibrating the SMA damper was assumed in tension condition and SMA wires made most of deformation of the damper neglecting residual martensite strain. As a result, the energy dissipated by SMA damper is significant. In order to simulate the SMA wire dampers in the building, the modified superelastic SMA wires model was implemented in ANSYS 16 (Parulekar et al. 2009).

In three-storey R.C.C structure, for all three stories of the building based on the damper capacity some adjustment is made which resulted in identical as SMA wire dampers. To understand the peak interstorey displacement along with the height of the building these adjustments are necessary. Therefore, the properties of SMA damper are length of the damper and area of damper were evaluated. In this study, the same set of parameters of SMA damper are used.

From last one decade, the finite element package ANSYS 10.0 has included the constitutive model proposed by Auricchio et al. (2001), to stimulate the superelastic

behavior of SMAs. Ansys software developed the one-dimensional constitutive model for superelastic SMAs is as shown in Figure 4.7. The SMA material behavior has three distinct transformation phases i.e., linear elastic an austenite phase, martensite phase and transition phase. To define stress-strain behavior of superelastic SMAs in loading and unloading for the uniaxial stress six sets of temperature dependent parameters are needed state as described in Table 4.5. Three-dimensional finite element models using the pseudoelastic constitutive model values described in the last section are used, the numerical simulations are performed with commercial finite element code ANSYS 2016. To describe pseudoelastic behavior through the incorporation of the Auricchio et al. (2001) constitutive model was considered. The presented numerical simulations considering the SMA mechanical component with the material properties are represented in Table 4.5.

Installation of SMA damper in building should be determined based on the two diagonal fixed points of building and each SMA damper should be determined. In this analysis, an SMA damper is placed diagonally between two points of each storey of the building. The parameter model should be determined to simulate the hysteresis behavior of SMA accurately. From the uniaxial test results, the elastic modulus E, the yield stress σ_y and the martensite finish strain ε_l were directly obtained and to define in SMA in software six material constants are required from C1 to C6 i.e. α, σ_s^{AS}, σ_f^{AS}, σ_s^{SA}, σ_f^{SA}, and E_A and ε_l are SMA wire material constants.

The boundary conditions at base of R.C.C structure is fixed. In this study, by several times of adjustments, the SMA damper is simplified as linear spring. The hysteric curve of SMA material model is the initial elastic stress-strain curve, the residual strain of NiTi wire is neglected. The material model of SMA is simulated using the superelastic material model of SMA, available in ANSYS material model library. At isothermal conditions, the superelastic SMA material, the stress–strain diagram given by Auricchio's model is as shown in Figure 4.10. Based on the test values of SMAs, the parameters are listed in Table 4.4 and stress strain behaviour of SMAs as shown in Figure 4.11 were used to simulate the SMA wire in ANSYS. The time history analysis of building with SMA damper is carried out under earthquake loading excitation and

are applied in X-direction. The response of the building in the form of lateral displacement and acceleration are determined.

Table 4.4 Material properties of shape memory alloy wire

Parameters	Value	Unit
Elastic moduli E_A	623.25	MPa
Austenite start stress σ_s^{AS}	754.46	MPa
Austenite finish stress σ_f^{AS}	454.71	MPa
Martensite start stress σ_s^{SA}	325.88	MPa
Martensite finish stress σ_f^{SA}	667	MPa
Transformation strain ε_l	4.5	%
α	0	-

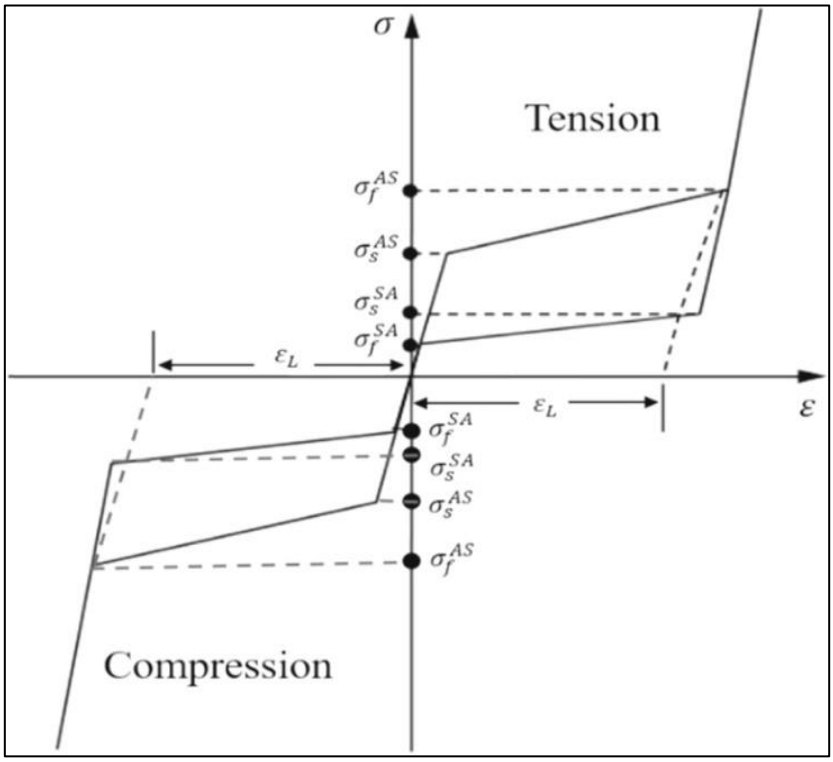

Figure 4.10 Cyclic stress–strain behavior of SMA (Auricchio 2001)

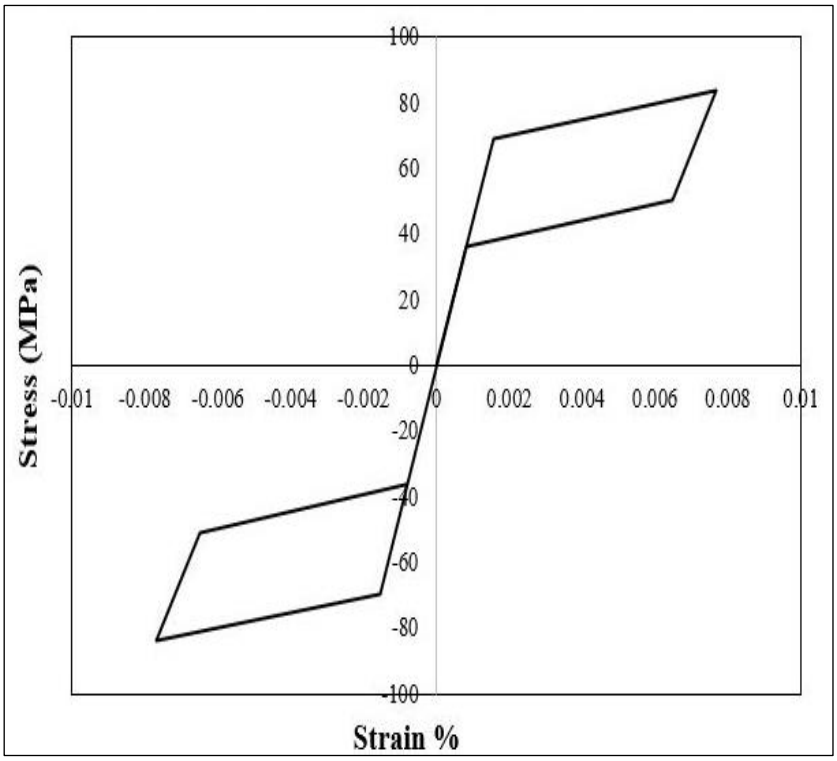

Figure 4.11 Stress-strain curve of SMA

Table 4.4 Shape memory alloy constants in ANSYS 10.0

Constants	Parameters
SIG-SAS(C1)	Starting stress value for the forward phase transformation Austenite start stress σ_s^{AS}
SIG-FAS(C2)	Final stress value for the forward phase transformation Austenite finish stress σ_f^{AS}
SIG-SSA(C3)	Starting stress value for the forward phase transformation Martensite start stress σ_s^{SA}
SIG-FSA(C4)	Final stress value for the forward phase transformation Martensite finish stress σ_f^{SA}
EPSILON(C5)	Maximum residual strain ε_l
ALPHA(C6)	Parameter measuring the difference between material response in tension and compression

4.7 Modelling of XPD and SMAD

The combined effect of XPD and SMAD devices placed in building are modelled by using bilinear elastic plastic material model. To evaluate the effect of yielding type X-plate damper and SMA wire damper in building, in the first phase of the analysis, the device has been defined in terms of linear spring. The equivalent linearization method is used for modelling and devices are designed in terms of elastic and hysteretic form, since it strongly affects the structural response demand throughout the analysis. The time history analysis was performed assuming building model as a single degree of freedom system. Repeating the analysis with combination of X-plate with thickness t=3mm and t=6mm and the property of SMA tabulated in Table 4.4 and the stress-strain characteristics of SMA is as shown in Figure 4.11.

Modelling the building system with combined effect taking into account the material parameters are tabulated in Table 4.3 and Table 4.5. The Elcentro scaled ground motion is used for the analysis with PGA value 0.1g and time step 0.02sec and 5% elastic damping ratio. The time history analysis of building with XPD and SMA damper is carried out under earthquake loading excitation are applied in X-direction. The response of the building is found out in terms of lateral displacement and acceleration.

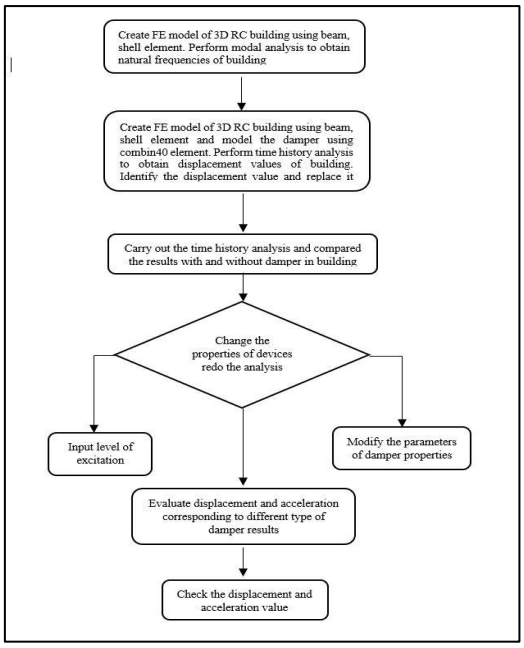

Figure 4.12 Flow chart of computational model

CHAPTER 5

RESULTS AND DISCUSSION

5.1 General

The analysis results of an uncontrolled building such as the natural frequency of the building and the building with damper models are presented in this chapter. The time history analysis is carried out with damper i.e. XPD, SMAD and XPD & SMAD and without damper in the building. Seismic analysis of three-dimensional R.C.C building is carried out using time history record of Elcentro ground motion. Building models with various damper configuration were analysed to find out the dynamic behaviour of structure with damper and the response of the building is compared within the different models. The results of seismic response of the structure with damper by the incorporation of the effect of stiffness, lateral displacement and acceleration and the variation in response of building with fixed base in comparison with conventional fixed base are also computed.

5.2 Fundamental Natural Period

Modal analysis has been carried out using commercially available FEM software. From the modal analysis, the dynamic characteristics such as time period and different mode shapes of the frame are obtained with a fixed condition at the base of the structure. It is seen that the first three modes excite 90% of the total mass. The number of modes to be considered is based on the criteria that the modal mass participation factor should be 90% or more and it will be satisfied by considering the first three modes of vibration. The natural frequencies of the model are tabulated in Table 5.1. The first three mode shapes of the uncontrolled 3D R.C.C structure obtained from the analysis is as shown in Figure 5.1.

Table 5.1 Natural frequencies at different modes of the structure

Mode No.	Frequency
1	4.871
2	5.731
3	7.443
4	15.561
5	18.882

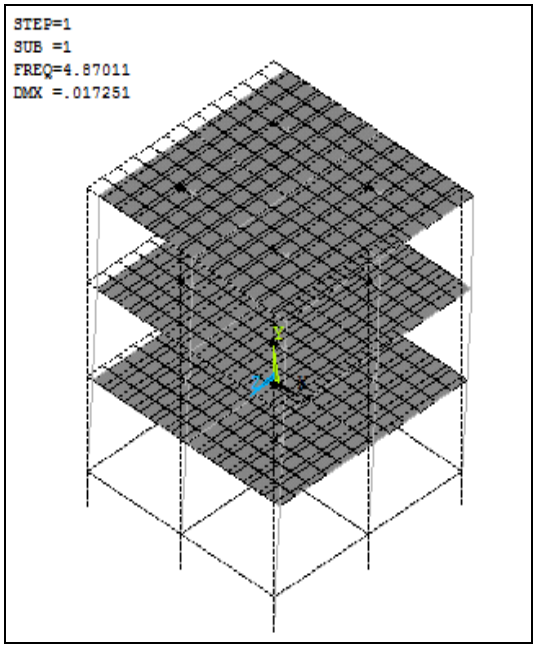

(a) Mode 1: f = 4.871Hz

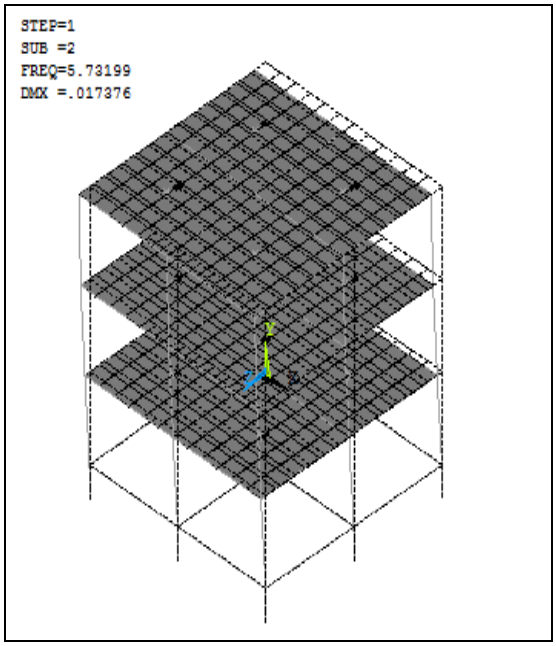

(b) Mode 2: f = 5.731 Hz

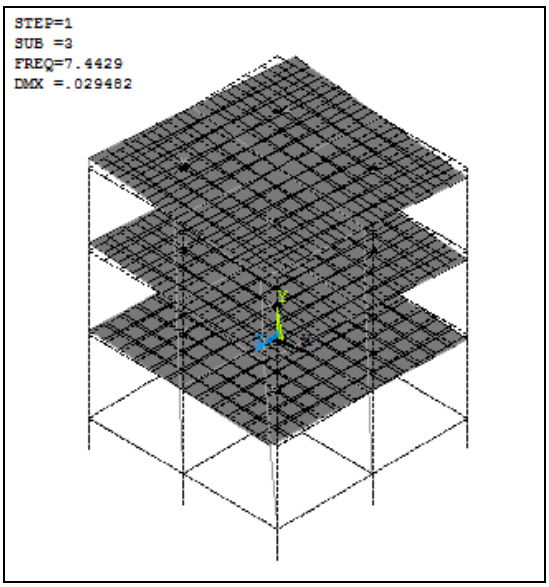

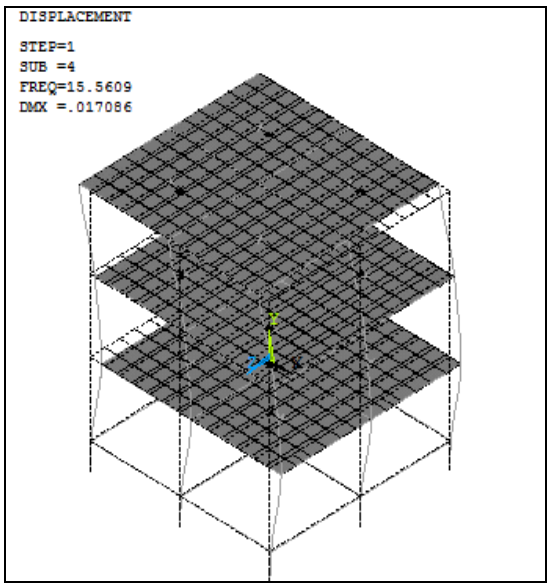

(c) Mode 3: f = 7.443 Hz **(d) Mode 4: f = 15.561 Hz**

Figure 5.1 Mode shapes of 3D RC structure

5.3 Time History Analysis

The time history analysis is carried out on building under earthquake ground motion. For the present study purpose, earthquake data of station Elcentro (1940) earthquake with its peak ground acceleration (PGA) scaled down to 0.1g and time interval of 0.02sec for the uncontrolled model as well as models with dampers (XPD, SMAD and XPD & SMAD) is analysed. The analysis has been carried out on the modified acceleration time histories that correspond to a scaled peak ground acceleration of 0.1g with a loading step at 0.02sec. Comparison is done for the response parameters such as displacement and acceleration of the building at different floor levels of the building and for each model respectively.

5.3.1 Effect of damper parameters on displacement

Displacement of all building models with dampers i.e. XPD, SMAD and XPD & SMAD and without damper is found from time history analysis and are tabulated. Reduction in displacement values due to dampers are studied. Variation in the displacement of building at different floor level are plotted.

To study the effect of the properties of the XPD thickness of the plate 't', height of the plate 'a' and breadth of the plate 'b' on the seismic response of the R.C.C building, the controlled system is analysed by varying the properties of the XPD, in the practical range of its size for different thickness (t) of XPD (3mm and 6mm). For each of the above parametric combinations, the building with damper system is analysed under Elcentro ground motion and the peak response quantities such as displacement and accelerations are plotted against the properties of the XPD with a=b=40mm and a=b=60mm respectively.

The results are listed in Table 5.2 and Table 5.3 for XPD of size a=b=40mm and a=b=60mm for two different thickness (i.e. t=3mm and t=6mm) respectively. The percentage reduction in displacement of the building system is also compared with various thickness of XPD. The peak response reduction of the building is noted under ground motion for the higher thickness of XPD. However, the response of the building under earthquake with a 6mm thick XPD slightly increased. The decrease in peak displacement response of the building with XPD is as shown in Figure 5.2 and Figure 5.3 respectively under earthquake.

Table 5.2 Comparison of displacement at different floor height of RC structure with and without XPD (t=3mm)

Displacement (mm)					
Floor Levels	**Without damper**	**With XPD (a=b=40mm)**	**With XPD (a=b=60mm)**	**% Reduction due to XPD**	
				With XPD (a=b=40mm)	**With XPD (a=b=60mm)**
Ground Floor	0.238	0.125	0.166	47.48	30.25
First Floor	2.535	0.818	1.354	67.73	46.59
Second Floor	4.412	1.284	2.181	70.90	50.57
Roof	5.361	1.519	2.609	71.67	51.33

Table 5.3 Comparison of displacement at different floor height of RC structure with and without XPD (t=6mm)

Displacement (mm)					
Floor Levels	**Without damper**	**With XPD (a=b=40mm)**	**With XPD (a=b=60mm)**	**% Reduction due to XPD**	
				With XPD (a=b=40mm)	**With XPD (a=b=60mm)**
Ground Floor	0.238	0.198	0.209	16.80	12.18
First Floor	2.535	1.987	2.156	21.61	14.95
Second Floor	4.412	3.471	3.714	21.32	15.82
Roof	5.361	4.342	4.633	19.01	13.57

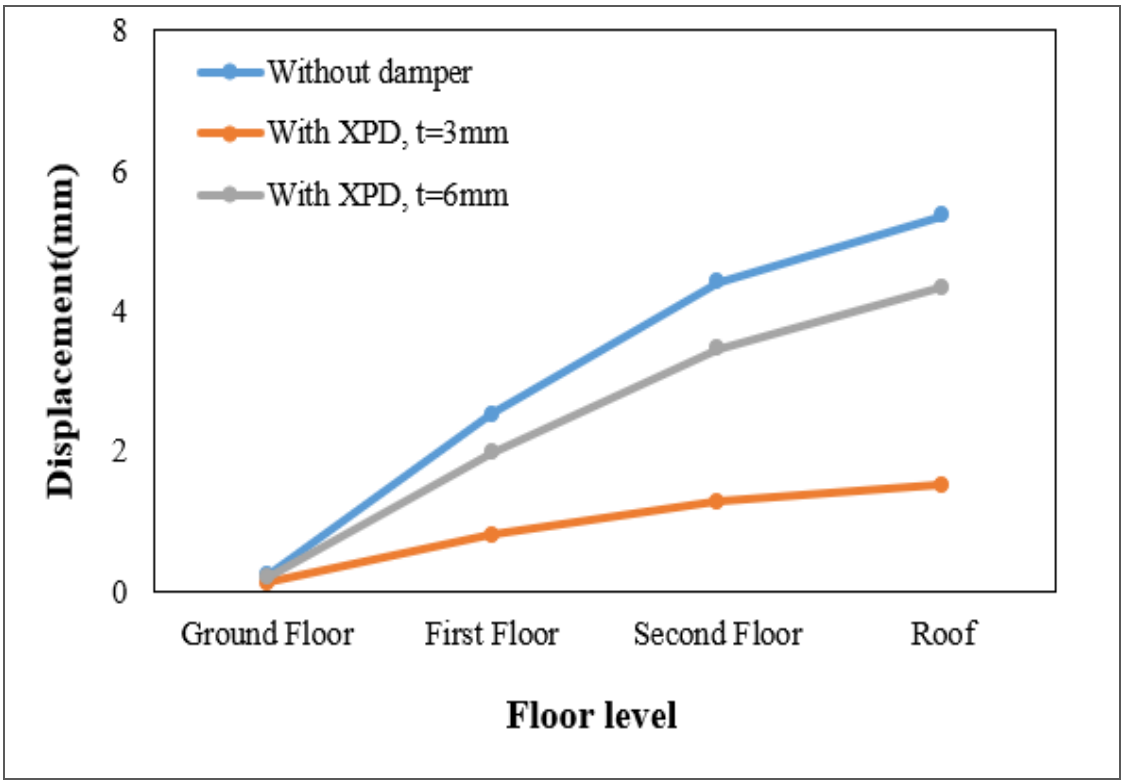

Figure 5.2 Comparison of floor level displacement at XPD (a=b=40mm)

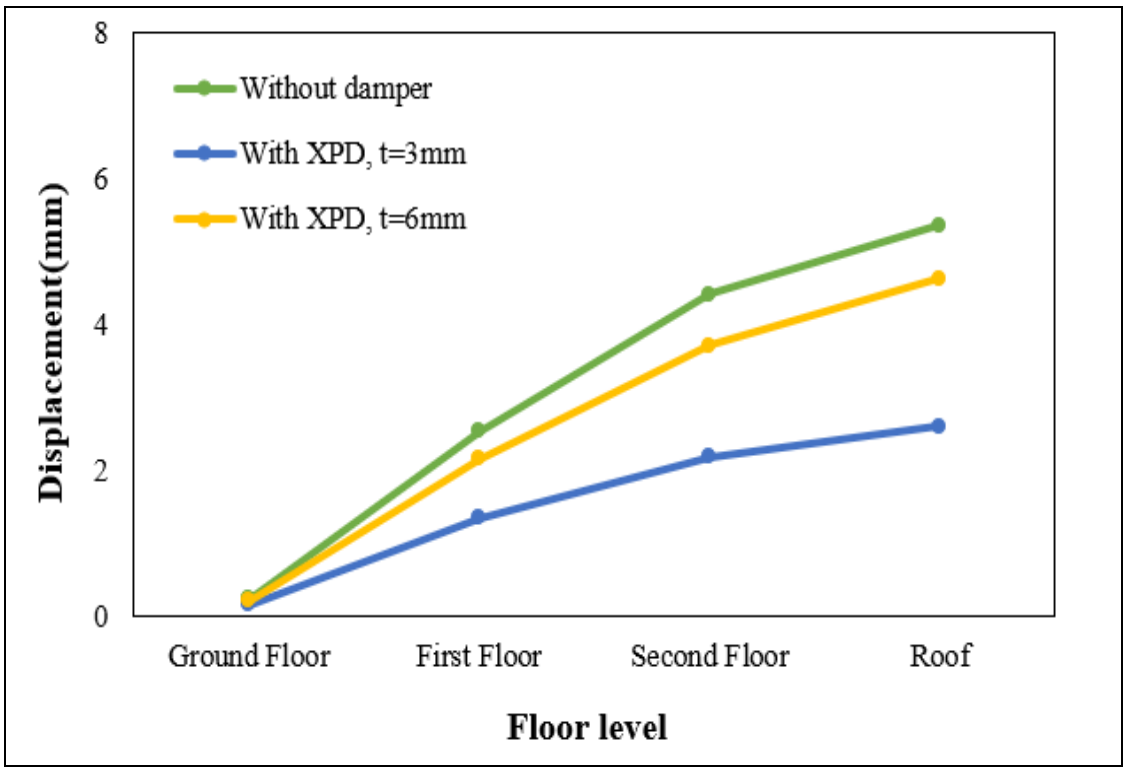

Figure 5.3 Comparison of floor level displacement at XPD (a=b= 60mm)

Figure 5.2 shows the variation in displacement response of the building against thickness t=3mm and t=6mm with size of X-plate a=b=40mm under Elcentro earthquake. The top floor displacement has been considerably reduced. 71.67% reduction is observed in the displacement of top floor. The reduction in second floor displacement is 70.90%, 67.73% is the reduction of displacement at first floor and 47.48% in ground floor with XPD having plate thickness t=3mm and plate size a=b=40mm in the building. Similarly, in the case of displacement of a building system with XPD having a=b=40mm, there is a reduction in displacement by 51.33% at top floor, 50.57% at the 2nd floor, 46.59% at the 1st floor and 30.25% at ground floor compared to the uncontrolled system under seismic event. This shows that, with an increase in floor height, there is considerable reduction in displacement. The displacement responses are very sensitive sizes of XPD 'a' and 'b' and it is observed that the response of the building reduced at smaller values of a=b=40mm. Similarly, it is observed in Figure 5.3, the variation of displacement over the height of the building with size of XPDs a=b=60mm and t=3mm and t=6mm. The displacement at top floor is reduced. The 19.01% reduction is observed in displacement of top floor. The

reduction in second, first and ground floor displacement is 21.32%, 21.61% and 16.80% respectively with XPD having plate thickness t=6mm and plate size a=b=40mm in the building. Similarly, in the case of displacement of a building system with XPD having a=b=60mm there is a reduction in displacement by 13.57% at top floor, 15.82% at the 2nd floor, 14.95% at the 1st floor and 12.18% at ground floor compared to the uncontrolled system under seismic event.

Energy dissipated by XPD is quickly reduced with increase in 'a' and 'b' values. It is noted from the Figure 5.2 and Figure 5.3, that XPDs are very effective in response of the uncontrolled building system. This indicates that XPDs are effective in reducing the response of the building. It is also observed that the seismic response of the RC building with varying for smaller values of 'a' and 'b' remains unaffected for further increase in the values of 'a' and 'b'. Moreover, the response of the building increases with increase in the thickness of the XPD. It is observed that further increase in the thickness of the XPD made building highly rigid thereby increasing the response values.

Table 5.4 Comparison of displacement at different floor height of RC structure with and without SMA

Floor Levels	Without damper	With SMA		% Reduction due to SMA	
		SMA1	SMA2	SMA1	SMA2
Ground Floor	0.238	0.214	0.223	10.08	6.30
First Floor	2.535	1.935	2.298	23.66	9.34
Second Floor	4.412	3.222	3.917	26.97	11.21
Roof	5.361	3.824	4.805	28.67	11.57

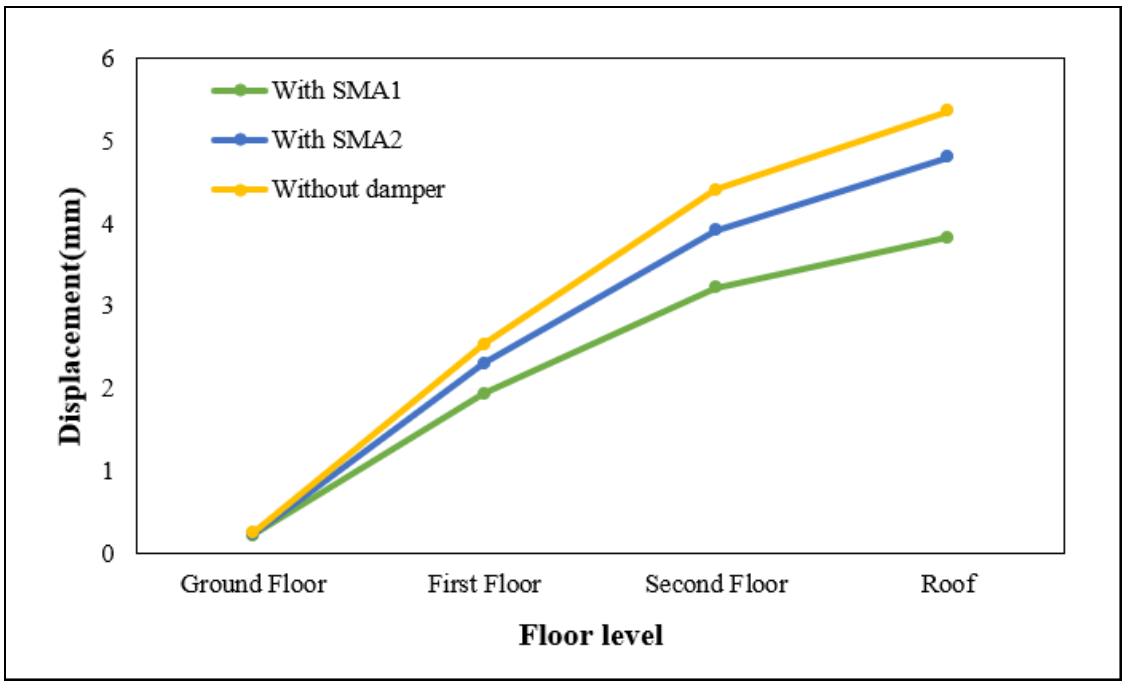

Figure 5.4 Comparison of floor level displacement of SMA

The response of the building at different floor height values of the building are tabulated in Table 5.4. Figure 5.4 represents the variation of displacement of the controlled with SMA damper and uncontrolled structure at different floor level of building system subjected to Elcentro earthquake ground motion of 0.1g PGA. It is found that at top floor 28.67% decrease in displacement is observed. The reduction in second floor displacement is 26.97%, 23.66% is the reduction in displacement at the first floor and 10.08% in the ground floor with SMA1 having wire diameter of 0.4mm in the building. Similarly, in case of displacement of a building system with SMA2 having diameter of wire 1.2mm there is reduction in displacement by 11.57% at top floor, 11.21% at the 2^{nd} floor, 9.34% at the 1^{st} floor and 6.30% at ground floor when compared to the uncontrolled system under seismic event. This shows that, with an increase in floor height, the displacement is reduced. Also, SMA2 is more effective compared to SMA1. From Figure 5.4, SMA1 (0.4mm diameter wire) damper, and SMA2 (1.2mm diameter wire) damper are very effective in reducing the seismic response of the building.

Table 5.5 Comparison of displacement at different floor height of RC structure with and without XPD and SMA at t=3mm

Displacement (mm)									
Floor Levels	**Without damper**	**With XPD (a=b=40mm) and SMA1**	**With XPD (a=b=60mm) and SMA1**	**With XPD (a=b=40mm) and SMA2**	**With XPD (a=b=60mm) and SMA2**	**% Reduction**			
						With XPD (a=b=40mm) and SMA1	**With XPD (a=b=60mm) and SMA1**	**With XPD (a=b=40mm) and SMA2**	**With XPD (a=b=60mm) and SMA2**
Ground Floor	0.238	0.105	0.119	0.122	0.137	55.88	50	48.74	42.44
First Floor	2.535	0.702	0.939	0.957	1.175	72.31	62.96	62.25	53.65
Second Floor	4.412	1.087	1.496	1.526	1.883	75.36	66.09	65.41	57.32
Roof	5.361	1.355	1.744	1.781	2.201	74.72	67.47	66.78	58.94

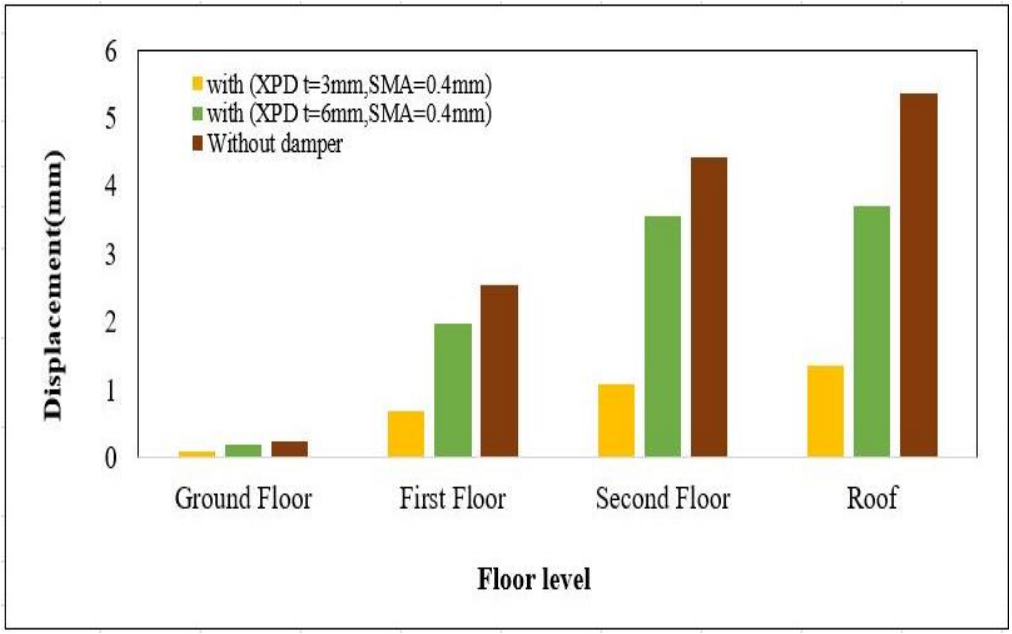

Figure 5.5 Comparison of floor level displacement of XPD and SMAD (a=b=40mm)

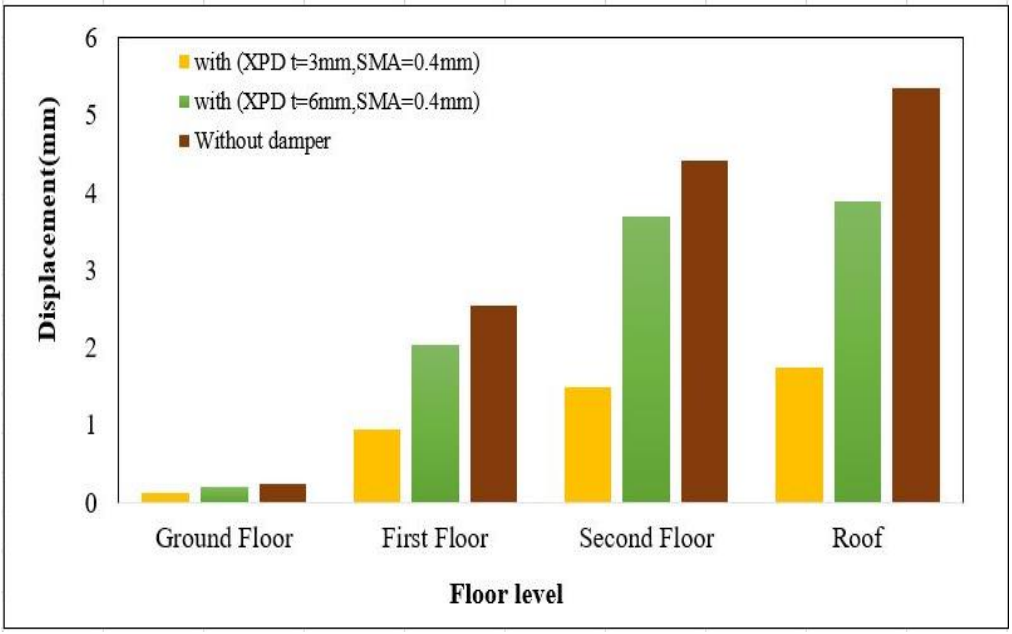

Figure 5.6 Comparison of floor level displacement of XPD and SMAD (a=b=60mm)

Figure 5.5 and Figure 5.6 shows the variation in response of displacement with the height of the building under seismic excitation with combined effect of damper. The floor displacement values of the building are tabulated in Table 5.5. The top floor displacement with XPD a=b=40mm and SMA1 the percentage reduction is 74.72%. It has been considerably reduced compared to SMA2 with XPD a=b=40mm. The reduction in second floor displacement is 75.36%. The percentage reduction in first floor and at the ground floor with XPD having plate thickness a=40mm and b=40mm with SMA1 and SMA2 in building is 72.31% and 55.88% respectively. Similarly, in building system with SMA device having wire diameter of 1.2mm, the reduction in displacement is observed in XPD of thickness a=b=60mm, SMA1 and SMA2 about 67.47% at top floor, 66.09% at the 2^{nd} floor, 62.96% at the first floor and 50% at ground floor reduced compared to the uncontrolled system under seismic event, due to the combined effect of the dampers in building under seismic excitation. This shows that, with increase in plate size of XPD a=b=60mm very small change in response of the building is observed.

Table 5.6 Comparison of displacement at different floor height of RC structure with and without XPD and SMA at t=6mm

Displacement (mm)									
Floor Levels	Without damper	With XPD (a=b=40mm) and SMA1	With XPD (a=b=60mm) and SMA1	With XPD (a=b=40mm) and SMA2	With XPD (a=b=60mm) and SMA2	% Reduction			
						With XPD (a=b=40mm) and SMA1	With XPD (a=b=60mm) and SMA1	With XPD (a=b=40mm) and SMA2	With XPD (a=b=60mm) and SMA2
Ground Floor	0.238	0.201	0.204	0.211	0.216	15.55	14.29	11.34	9.24
First Floor	2.535	1.968	2.039	2.121	2.166	22.37	19.57	16.33	14.56
Second Floor	4.412	3.565	3.695	3.728	3.828	19.20	16.25	15.50	13.24
Roof	5.361	3.717	3.892	4.334	4.498	30.67	27.40	19.16	16.10

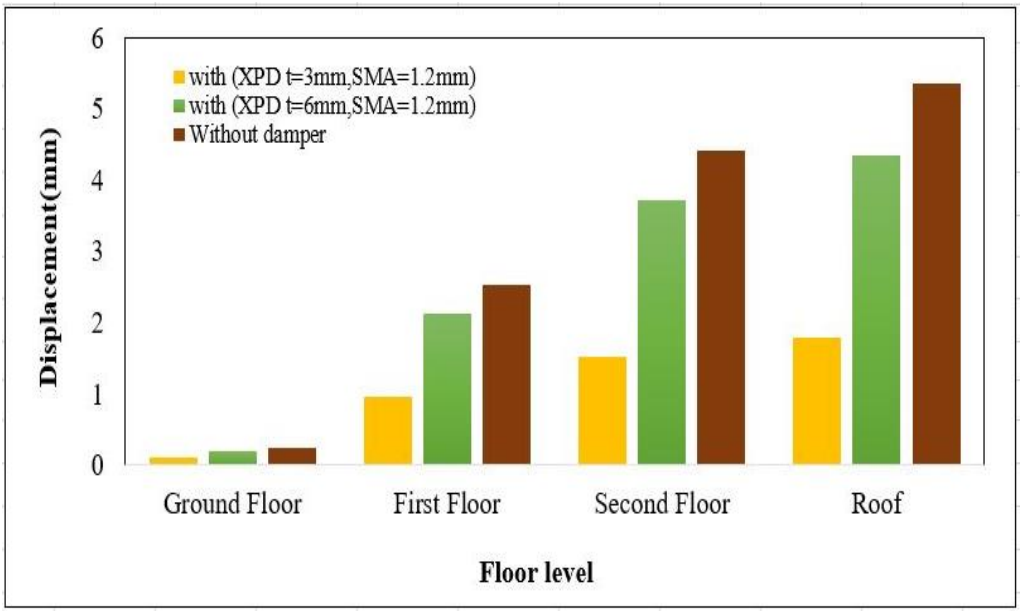

Figure 5.7 Comparison of floor level displacement of XPD and SMAD (a=b=40mm)

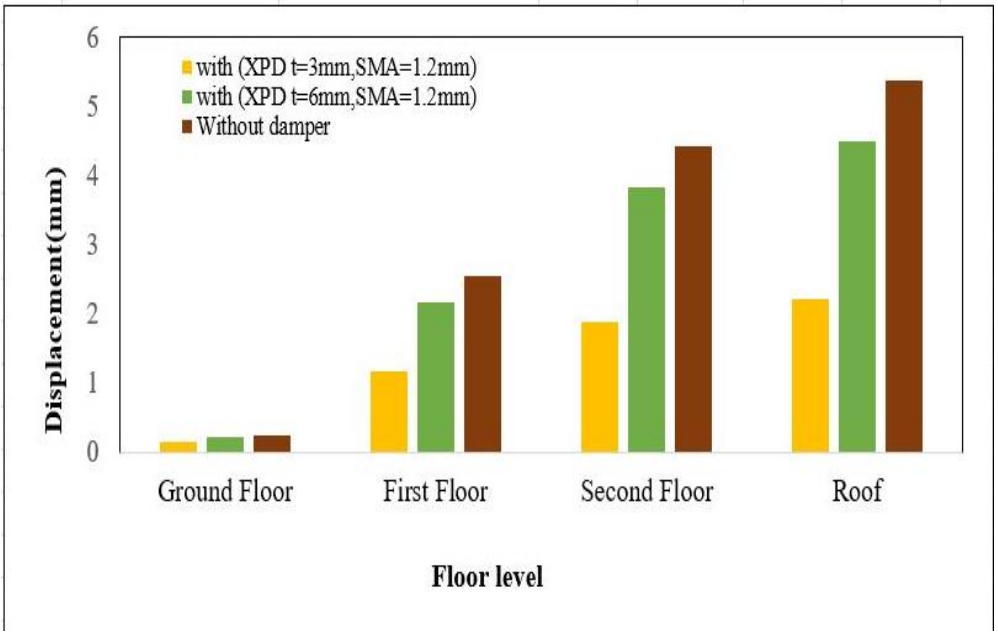

Figure 5.8 Comparison of floor level displacement of XPD and SMAD (a=b=60mm)

Figure 5.7 and Figure 5.8 show the variation in response of displacement with the top floor of the building under seismic excitation with combined effect of XPD and SMAD. In this case the thickness of XPD is considered as t=6mm. The floor displacement values of the building are tabulated in Table.5.5. The top floor displacement with XPD a=b=40mm and SMA1 the percentage reduction is 30.67% has been considerably

reduced compared with SMA2 with XPD a=b=40mm. The reduction in second floor displacement is 19.20%. 22.37% is the reduction of first floor and 15.55 % at the ground floor with XPD having plate thickness a=40mm and b=40mm with SMA1 and SMA2 in the building. Similarly, in case of displacement of a building system with SMA device having a wire diameter of 1.2mm there is a reduction in XPD a=b=60mm SMA1 and SMA2 displacement by 27.40% at top floor, 16.25% at the 2nd floor, 19.57% at the first floor and 14.29% at ground floor reduced compared to the uncontrolled system under earthquake ground motion. This shows that, with an increase in plate thickness t=6mm of XPD there is not much change observed in response of the building.

5.3.2 Effects of damper parameter on acceleration

Acceleration values of building with and without damper of all building models are obtained using time history analysis. Reduction in these values, due to addition of dampers are analysed. The obtained results are tabulated. The variation in acceleration at various height of the building are plotted accordingly.

Table 5.7 Comparison of acceleration at different floor height of RC structure with and without XPD (t= 3mm)

Acceleration (m/s^2)					
Floor Levels	**Without damper**	**With XPD (a=b=40mm)**	**With XPD (a=b=60mm)**	**% Reduction**	
				With XPD (a=b=40mm)	**With XPD (a=b=60mm)**
Ground Floor	0.315	0.237	0.251	24.76	20.32
First Floor	2.663	2.352	2.389	11.68	10.29
Second Floor	3.972	3.765	3.773	5.21	5.01
Roof	5.531	5.312	5.517	3.96	0.25

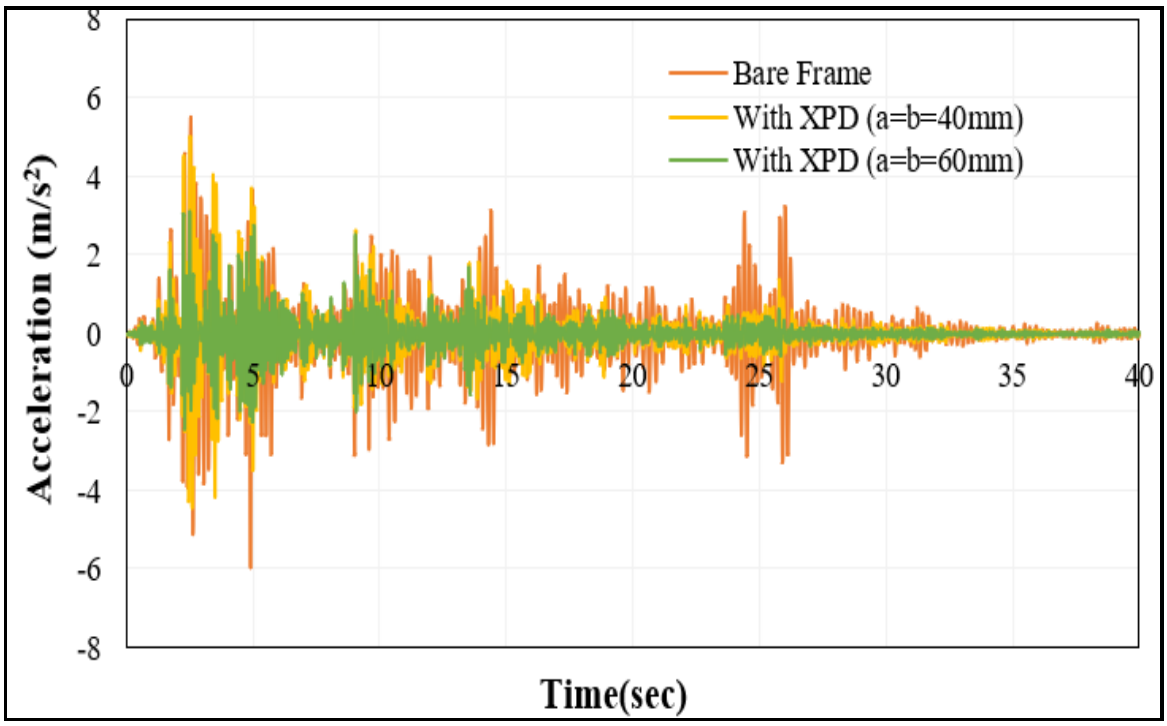

Figure 5.9 Variation in acceleration at top floor with XPD (t=3mm)

Figure 5.9 show the variation of response acceleration with the top floor of the building under seismic excitation. The floor acceleration values of the building are tabulated in Table 5.7. The top floor acceleration has been considerably reduced. The 3.96% reduction is observed in acceleration of top floor. The reduction in second floor acceleration is 5.21%, 11.68% is the reduction in acceleration at the first floor and 24.76% in the ground floor with XPD having plate thickness t=3mm and plate size a=b=40mm in the building. Similarly, in case of acceleration of a building system with XPD having a=b=60mm there is a reduction in acceleration by 0.25% at top floor, 5.01% at the 2nd floor, 10.29% at the 1st floor and 20.32% at ground floor reduced when compared to the uncontrolled system under seismic event.

Table 5.8 Comparison of acceleration at different floor height of RC structure with and without XPD (t= 6mm)

Acceleration (m/s^2)					
Floor Levels	**Without damper**	**With XPD (a=b=40mm)**	**With XPD (a=b=60mm)**	**%Reduction**	
				With XPD (a=b=40mm)	**With XPD (a=b=60mm)**
Ground Floor	0.315	0.215	0.285	31.75	9.52
First Floor	2.663	1.769	2.009	33.57	24.56
Second Floor	3.972	3.404	3.581	14.30	9.84
Roof	5.531	4.436	4.736	19.80	14.37

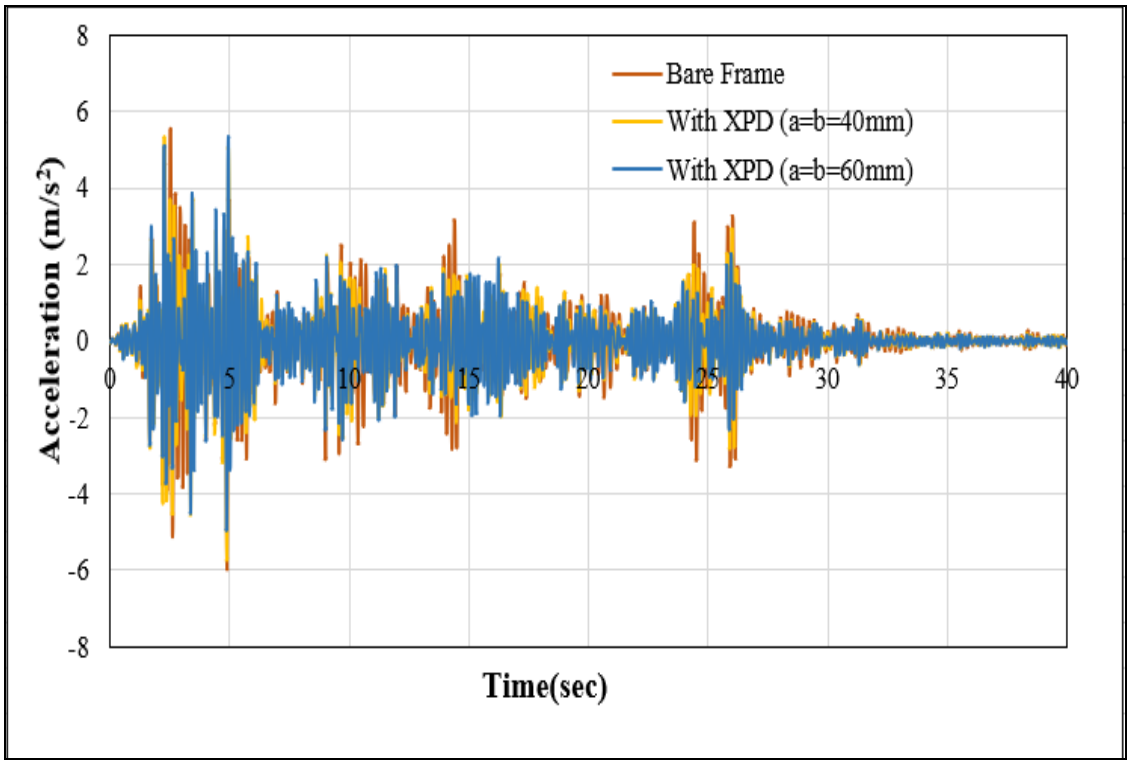

Figure 5.10 Variation in acceleration at top floor of XPD (t=6mm)

Figure 5.10 shows the variation in response of peak acceleration of top floor of the building under seismic excitation. The floor acceleration values of the building are tabulated in Table.5.8. The top floor acceleration has been considerably reduced.

19.80% reduction is observed in acceleration of top floor. The reduction in second floor acceleration is 14.30%, 33.57% is the reduction of acceleration at the first floor and 31.75% in the ground floor with XPD having plate thickness t=6mm and plate size a=b=40mm in the building. Similarly, in the case of acceleration of a building system with XPD having a=b=60mm there is a reduction in acceleration by 14.37% at top floor, 9.84% at the 2nd floor, 24.56% at the 1st floor and 9.52% at ground floor reduced compared to the uncontrolled system under seismic event.

Table 5.9 Comparison of acceleration at different floor height of RC structure with and without SMA

Acceleration (m/s^2)					
Floor Levels	**Without damper**	**With SMA1**	**With SMA2**	**% Reduction**	
				SMA1	**SMA2**
Ground Floor	0.315	0.257	0.268	18.41	14.92
First Floor	2.663	2.401	2.443	9.84	8.26
Second Floor	3.972	4.142	3.816	4.28	3.93
Roof	5.531	5.249	5.034	8.98	5.10

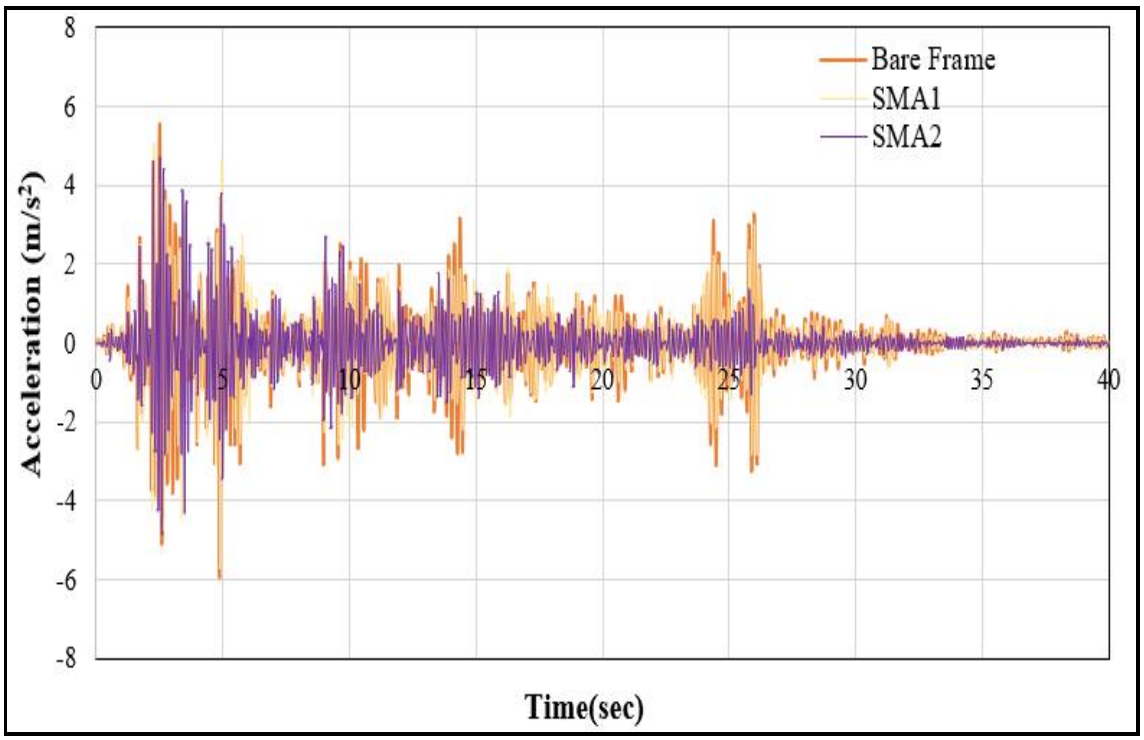

Figure 5.11 Variation in acceleration at top floor with SMA

Figure 5.11 shows the variation in response of acceleration with the top floor of the building under seismic excitation. The floor acceleration values of the building are tabulated in Table 5.9. The top floor acceleration has been considerably reduced. 8.98% reduction is observed in acceleration of top floor. The reduction in second floor acceleration is 4.28%, 9.84% is the reduction of acceleration at the first floor and 18.41% in the ground floor with SMA1 having diameter of wire 0.4mm in the building. Similarly, in the case of acceleration of a building system with SMA2 having diameter of wire 1.2mm there is a reduction in acceleration by 5.10% at top floor, 3.93% at the 2nd floor, 8.26% at the 1st floor and 14.92% at ground floor reduced compared to the uncontrolled system under seismic event. SMA1 is more effective compared to SMA2.

Table 5.10 Comparison of acceleration at different floor height of RC structure with and without XPD and SMA (t= 3mm)

Acceleration (m/s^2)									
Floor Levels	**Without damper**	**With XPD (a=b=40mm) and SMA1**	**With XPD (a=b=60mm) and SMA1**	**With XPD (a=b=40mm) and SMA2**	**With XPD (a=b=60mm) and SMA2**	**% Reduction**			
						With XPD (a=b=40mm) and SMA1	**With XPD (a=b=60mm) and SMA1**	**With XPD (a=b=40mm) and SMA2**	**With XPD (a=b=60mm) and SMA2**
Ground Floor	0.315	0.213	0.223	0.254	0.267	32.38	29.21	19.37	15.24
First Floor	2.663	1.852	1.921	2.401	2.436	30.45	27.86	9.84	8.52
Second Floor	3.972	3.246	3.539	3.805	3.821	18.28	10.90	4.20	3.80
Roof	5.531	4.136	4.388	4.714	5.011	25.22	20.67	14.77	9.40

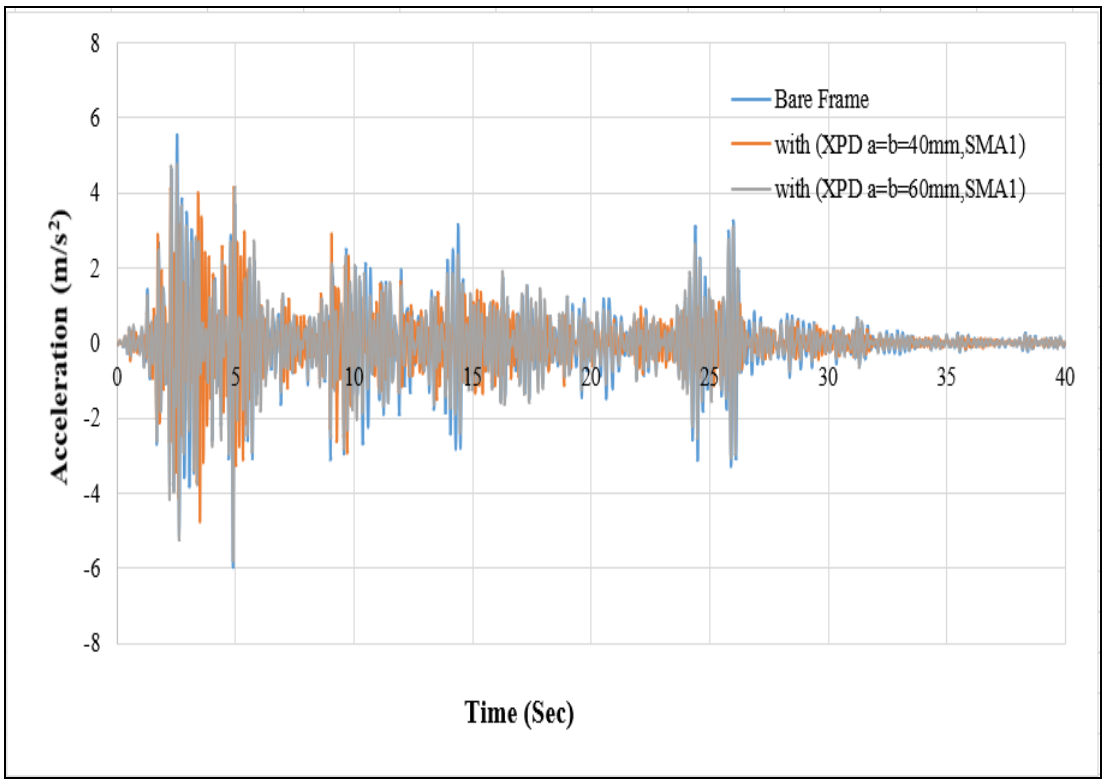

Figure 5.12 Variation in acceleration at top floor of XPD and SMA1 (t=3mm)

Figure 5.12 shows the variation in response of acceleration with the top floor of the building under seismic excitation. The floor acceleration values of the building are tabulated in Table 5.10. The top floor acceleration with XPD a=b=40mm and SMA1, the reduction is 25.22% compared with SMA2 with XPD a=b=40mm. The reduction in second floor acceleration is 18.28%. 30.45% is the reduction of first floor and 32.88 % at the ground floor with XPD having plate thickness a=40mm and b=40mm with SMA1 in the building. Similarly, in the case of acceleration of a building system with SMA device having a wire diameter of 1.2mm there is a reduction in XPD a=b=60mm SMA1 acceleration by 20.67% at top floor, 10.90% at the 2nd floor, 27.86% at the first floor and 29.21% at ground floor reduced compared to the uncontrolled system under seismic event, due to the combined effect of the dampers in the building under seismic excitation.

Table 5.11 Comparison of acceleration at different floor height of RC structure with and without XPD and SMA (t= 6mm)

Acceleration (m/s^2)									
Floor Levels	**Without damper**	**With XPD (a=b=40mm) and SMA1**	**With XPD (a=b=60mm) and SMA1**	**With XPD (a=b=40mm) and SMA2**	**With XPD (a=b=60mm) and SMA2**	**% Reduction**			
						With XPD (a=b=40mm) and SMA1	**With XPD (a=b=60mm) and SMA1**	**With XPD (a=b=40mm) and SMA2**	**With XPD (a=b=60mm) and SMA2**
Ground Floor	0.315	0.232	0.249	0.257	0.291	26.35	20.95	18.41	7.62
First Floor	2.663	1.936	2.129	2.412	2.443	27.30	20.05	9.43	8.26
Second Floor	3.972	3.566	3.544	3.828	4.181	10.22	10.78	3.63	5.26
Roof	5.531	4.208	4.417	4.903	5.314	23.92	20.14	11.35	3.92

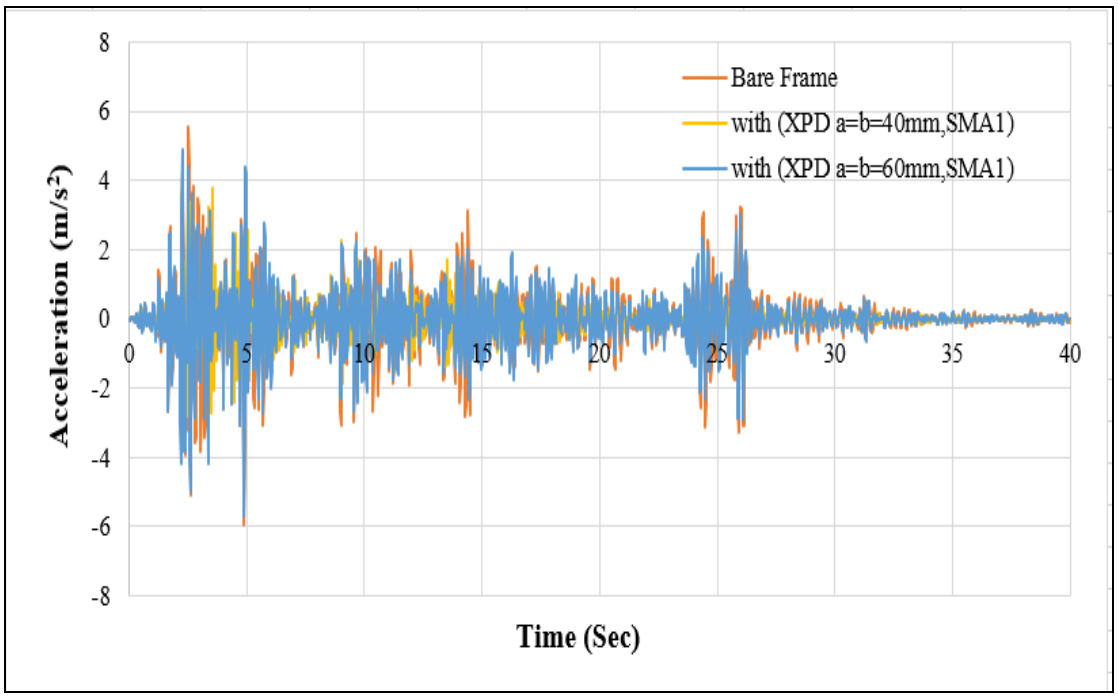

Figure 5.13 Variation in acceleration at top floor of XPD and SMA1 (t=6mm)

Figure 5.13 shows the variation of response acceleration with top floor of the building under seismic excitation. The floor acceleration values of the building are tabulated in Table 5.11. The top floor acceleration with XPD a=b=40mm and SMA1 the reduction is 23.92% has been considerably reduced compared with SMA2 with XPD a=b=40mm. The reduction in second floor acceleration is 10.22%, 27.30% is the reduction of first floor and 26.35% at the ground floor with XPD having plate thickness a=40mm and b=40mm with SMA1 and SMA2 in the building. Similarly, in case of acceleration of a building system with SMA device having wire of diameter of 1.2mm there is a reduction in XPD a=b=60mm SMA1 and SMA2 acceleration by 20.14% at top floor, 10.78% at the 2nd floor, 20.05% at the first floor and 20.95% at ground floor reduced compared to the uncontrolled system under seismic event, due to the combined effect of the dampers in the building under seismic excitation.

CHAPTER 6

CONCLUSIONS

6.1 Conclusions

The analysis of three-dimensional RC building was carried out with XPD, SMAD and XPD & SMAD, comparison was done with the dynamic behaviour of building model without damper using time history record. The input acceleration of El Centro ground motion having PGA value 0.1g was considered. Based on the present study the following conclusions are drawn:

- In the modal analysis it is found that the natural frequency of the building without damper is 4.871Hz and it increases with XPD is 5.27Hz, SMAD with 5.51Hz and also combined effect of (XPD & SMAD) is 6.12Hz dampers in the building. It is observed that the stiffness of the building also increases with dampers.

- The top floor, second floor, first floor and ground floor displacement and acceleration response of building with XPD, SMAD and combination of XPD & SMAD dampers subjected to earthquake ground motion using ANSYS version 16 analytical model is analysed. It is observed that, with the damper in the building, there is a significant response reduction of building with XPDs, SMAs and combination of XPD and SMAD dampers when compared with the conventional building.

- Reduction in peak response of the building has been observed with higher plate thickness i.e. t=6mm and different size of XPD but with the increase in size of plate i.e. a=b=60mm there no much changes observed in the response of building.

- With regard to XPD having plate thickness a=b=40mm and thickness of XPD is t=3mm and t=6mm, has significant reduction in response building when compared with the XPD having plate size a=b=60mm.

- Similarly, when SMA wire of diameter 0.4mm damper is used in the building, there is an additional decrease in displacement compared to 1.2mm diameter SMA wire damper and XPDs. Based on the results, it is concluded that the application of SMA damper in seismic analysis of building is possible and can lead to several advantages. SMA dampers are characterized by energy dissipation and numerical investigations have illustrated that it is comparable for its effect on the response to the dissipation of actual very high amount of energy dissipating devices.

- Finally, it is concluded that the combination of XPD and SMA damper provides the most effective in seismic response control of building under earthquake loading with XPD of thickness t=3mm and t=6mm having size of plate a=b=40mm and SMA wire of diameter 0.4mm.

- In the present research work, it is concluded that application of dampers in a building increases the stiffness of the entire building structure depending upon the size and parameters of dampers used. Also, the stiffness of each damper in a building will significantly affect the free vibration characteristics of the building.

6.2 Scope of Future Work

1) To verify the performance of building of the proposed method, it is suggested to conduct experiments under different dynamic loading conditions.

2) To increase the efficiency of building under dynamic loading with damper, optimization techniques can be used.

3) The experimental studies may be carried out for the scaled model of actual concrete and steel building in order to analyze the results obtained during the numerical simulation.

REFERENCES

Aiken, I.D., Nims, D.K., and Kelly, J.M., (1992). "Comparative study of four passive energy dissipation systems." *Bulletin of the New Zealand Society for Earthquake Engineering*, *25*(3), 175-192.

ANSYS Commands Reference, (2016). ANSYS release notes Inc., http:/www.ansys.com.

Auricchio, F., (2001). "A robust integration-algorithm for a finite-strain shape-memory-alloy superelastic model." *International Journal of plasticity*, *17*(7), 971-990.

Asgarian, B., and Moradi, S., (2011). "Seismic response of steel braced frames with shape memory alloy braces." *Journal of Constructional Steel Research*, 67(1), 65-74.

Azadi, B., Rajapakse, R. K. N. D., and Maijer, D. M., (2006). "Multi-dimensional thermomechanical model for pseudoelastic response of SMA." In *smart structures and materials, modeling, signal processing, and control" International* Society for Optics and Photonics. 616(6), 61660Y.

Bakre, S.V., Jangid, R. S., and Reddy, G. R., (2006). "Optimum X-plate dampers for seismic response control of piping systems." *International Journal of Pressure Vessels and Piping*, 83(9), 672–685.

Baratta, A., and Corbi, O., (2002). "On the dynamic behaviour of elastic–plastic structures equipped with pseudoelastic SMA reinforcements." *Computational Materials Science*, *25*(1-2), 1-13.

Basker, R. P., and Jangid, R. S., (2001). "Experimental study of base-isolated structures." *ISET journal of earthquake Technology*, *38*(1), 1-15.

Boyd, J. G., and Lagoudas D. C., (1996). "Thermodynamical constitutive model for shape memory materials: Part I. the monolithic shape memory alloy." *International Journal of Plasticity*, 12(6), pp.805–842.

Boyd, J. G., and Lagoudas, D. C., (1996). “Thermodynamical constitutive model for shape memory materials. Part II. The SMA composite material.” *International Journal of Plasticity*, *12*(7), 843-873.

Bruno, S., and Valente, C., (2002). “Comparative response analysis of conventional and innovative seismic protection strategies.” *Earthquake Engineering and Structural Dynamics*, 31(5), 1067-1092.

Brinson, L. C., (1993). “One - dimensional constitutive behavior of shape memory alloys: Thermo mechanical derivation with non-constant material functions and redefined martensite internal variable.” *Journal of Intelligent Material Systems and Structures*, 4(2), 229–242.

Bruno, S., and Valente, C., (2002). “Comparative response analysis of conventional and innovative seismic protection strategies.” *Earthquake Engineering and Structural Dynamics*, 31(5), 1067-1092.

Buehler, W.J., and Wang F.E., (1968). “A summary research in the nitinol alloys and their potential applications in ocean engineering.” *Ocean Engineering*, 1(1), 105-120.

Carboni, B., Lacarbonara, W., and Auricchio, F., (2015). “Hysteresis of multiconfiguration assemblies of nitinol and steel strands: experiments and phenomenological identification.” *Journal of Engineering Mechanics*, *141*(3), 0401-4135.

Caracoglia, L., and Jones, N. P., (2007). “Passive hybrid technique for the vibration mitigation of systems of interconnected stays.” *Journal of Sound and Vibration*, *307* (3-5), 849-864.

Casciati, F, Faravelli L., and Al Saleh, R., (2009). “An SMA passive device proposed within the highway bridge benchmark.” *Journal of Structural Control and Health Monitoring*, 16(6), 657 – 667.

Caughey, T.K., (1960). “Sinusoidal Excitation of a system with Bilinear Hysterisis.” *ASME Journal of Applied Mechanics*. 27, 640-643.

Chang, L. C., and Read, T. A., (1951). “Plastic deformation and diffusion less phase changes in metals—The gold-cadmium beta phase.” *Journal of Mechanics, 3*(1), 47-52.

Charney, F. A., Symans, M. D., Whittaker, A. S., Constantinou, M. C., Kircher, C. A., Johnson, M. W., and McNamara, R. J., (2008). “Energy dissipation systems for seismic applications: current practice and recent developments.” *Journal of structural engineering, 134*(1), 3-21.

Chethan, K, R. Ramesh Babu, Katta Venkataramana and Akanshu Sharma (2009), “Study on Dynamic Characteristics of 3D Reinforced Concrete Frame with Masonry infill”, Journal of CPRI, Bangalore.

Chopra, A. K., (2001). “*Dynamics of Structures, Theory and Application to Earthquake Engineering*.” Prentice Hall of India Pvt. Limited, New Delhi.

Constantinou, M. C., Soong, T.T., and Dargush, G. F., (1998). “Passive energy dissipation systems for structural design and retrofitt.” *Monograph No. 1. Buffalo (NY): Multidisciplinary Center for Earthquake Engineering Research.*

Curadelli, R. O., and Riera, J. D., (2004). “Reliability-based assessment of the effectiveness of metallic dampers in buildings under seismic excitations.” *Engineering Structures*, 26(13), 1931–1938.

Darel, E. H., (1990). “Shape memory alloy ASM Handbook, Volume 2: Properties and Selection: Nonferrous Alloys and Special-Purpose Materials.” *ASM Handbook Committee*, 1119-1124.

Desroches, R. and Smith, B., (2004). “Shape memory alloys in seismic resistant design and retrofit: A critical review of their potential and limitations.” *Journal of Earthquake Engineering*, 8(3), 415-429.

DesRoches, R., McCormick J., and Delemont, M., (2004). “Cyclic Properties of Super-elastic Shape Memory Alloy Wires and Bars.” *Journal of Structural and Engineering*, 130(1), 38-46.

Dezfuli, F. H., and Alam, M. S., (2013). “Shape memory alloy wire-based smart natural rubber bearing.” *Smart Materials and Structures*, *22*(4), 045-013.

Dolce, M., Cardone, D. and Marnetto, R., (2000). “Implementation and testing of passive control devices based on shape memory alloys.” *Earthquake Engineering and Structural Dynamics*, *29*(7), 945-968.

Dolce, M., and Cardone, D., (2001). “Mechanical behaviour of shape memory alloys for seismic applications 2. Austenite NiTi wires subjected to tension.’’ *International Journal of Mechanical Sciences*, *43*(11), 2631-2656.

Dolce, M., and Cardone, D., (2001). “Mechanical behaviour of shape memory alloys for seismic applications 2. Austenite NiTi wires subjected to tension.” *International Journal of Mechanical Sciences*, *43*(11), 2657-2677.

Ghodke, S., and Jangid, R.S., (2016). “Influence of high austenite stiffness of shape memory alloy on the response of base-isolated benchmark building.” *Structural Control and Health Monitoring*, *24*(2), e1867.

Graesser, E. J., and Cozzarelli, F. A., (1991). “Shape-memory alloys as new materials for aseismic isolation.” *Journal of Engineering Mechanics*, 117(11), 2590–2608.

Gur, S., Mishr, S. K., Chakraborty, S., (2014). “Performance assessment of buildings isolated by shape-memory-alloy rubber bearing: Comparison with elastomeric bearing under near-fault earthquakes.” *Structural Control and Health Monitoring,* 21(4), 449-65.

Hashemi, S.M.T., and Khadem, S.E., (2006). “Modeling and analysis of the vibration behavior of a shape memory alloy beam.” *International Journal of Mechanical Science*, 48(1), 44–52.

He, X. M., Rong, L. J., Yan, D. S., and Li, Y. Y., (2005). “Temperature memory effect of Ni47Ti44Nb9 wide hysteresis shape memory alloy.” *Scripta materialia*, *53*(12), 1411-1415.

Housner, G.W., Bergman, L.A., Caughey, T., Chassiakos, A., Claus, R., Masri, S., Skelton, R., Soong, T., Spencer, B., and Yao, J., (1997). "Structural control: past, present, and future." *Journal of Engineering Mechanics*., 123(9), 897-971.

IS 1893 - 2016 "Indian Standard, Criteria for earthquake resistant design of structures, Part I: General provisions and buildings", (Fifth revision., 2016)

IS 13920 - 2016 "Ductile design and detailing of reinforced concrete structures subjected to seismic forces code of practices", (First Revision 2016)

Jason, M., S.M., Reginald, D., Davide, F. and Ferdinando, A., (2007). "Seismic assessment of concentrically braced steel frames with shape memory alloy braces." *Journal of Structural Engineering*, 133(6), 862–870.

Justin, O., Reginald, D., Roberto, T. L., Gregory Hess, W., Robert, K., Jack, R. H., and Steve, S., (2004). "Steel beam-column connections using shape memory alloys." *Journal of Structural Engineering*, 130(5), 732–740.

Kareem, A., (1997). "Modelling of base-isolated buildings with passive dampers under winds." *Journal of Wind Engineering and Industrial Aerodynamics*, *72*(1), 323-334.

Kelly, J.M, Skinner, R.I and Heine, A.J., (1972). "Mechanisms of energy absorption in special devices for use in earthquake resistant structures." *Bull NZ Soc Earthquake Engineering*, 5(3) 63-73.

Lexcellent, C, and Bourbo, G., (1996). "Thermo-dynamical model of cyclic behaviour of Ti-Ni and Cu-Zn-A1 shape memory alloys under isothermal undulated tensile tests." *Mechanics of Materials,* 24(1), 59-73.

Liu, N., and Huang, W. M., (2006). "DSC study on temperature memory effect of NiTi shape memory alloy." *Transactions of Nonferrous Metals Society of China*, *16*, 37-41.

Liang, C. and Rogers C.A., (1992). "A multi-dimensional constitutive model for shape memory alloys." *Journal of Engineering Mathematics*, 26(3), 429–443.

Liu, Y, and Xiang, H., (1998) “Apparent modulus of elasticity of near-equiatomic NiTi.” *Journal of Alloys and Compounds*, 270(1-2),154-159.

Malecot, P., Lexcellent, C., Foltete, E., and Collet, M., (2006). “Shape memory alloys cyclic behavior: experimental study and modeling.” 128(3), 335-345.

Matthew, S., Darel. E., Hodgson, Reginald, D., and Roberto, T. L., (2009). “Shape memory alloy tension/compression device for seismic retrofit of buildings.” *Journal of Materials Engineering and Performance*, 18(5-6), 746– 753.

Marshall, J. D., and Charney, F. A., (2010a). “A hybrid passive control device for steel structures, I: development and analysis.” *Journal of Constructional Steel Research*, 66(10), 1278-1286.

Marshall, J. D., and Charney, F. A., (2010b). “A hybrid passive control device for steel structures, II: Physical testing”, *Journal of Constructional Steel Research*, 66(10), 1287-1294.

McCormick, J., Barbero, L., and DesRoches, R., (2006). “Effect of mechanical training on the properties of superelastic shape memory alloys for seismic applications.” *Proc. SPIE*, 5764, 430–439.

McCormick, J., Tyber, J., DesRoches, R., Gall, K., and Maier, H. J., (2007). “Structural engineering with NiTi. II: mechanical behavior and scaling.” *Journal of Engineering Mechanics*, *133*(9), 1019-1029.

Michael, D., and Michael, C. C., (1999). “Semi-active control systems for seismic protection of structures: A state-of-the-art review.” *Engineering Structures*, 21(6), 469–487.

Miyazaki, S., Sugaya Y., and Otsuka, K., (1988). “Effects of various factors on fatigue life of Ti–Ni alloys.” *Proc. MRS International. Meeting. on Advanced material*, Tokyo, Japan, May–June, 9, 251–256.

Miyazaki, S., Igo, Y., and Otsuka, K., (1986). “Effect of thermal cycling on the transformation temperatures of Ti- Ni alloys”. *Acta Metallurgica*, *34*(10), 2045-2051.

Mohamed, O., (2014). “Seismic response of braced steel frames with shape memory alloy and mega bracing systems”. *International Journal of Civil, Architectural Science and Engineering*, *8*(2), 131-138.

Motahari, S.A., Ghassemieh, M. and Abolmaali, S.A., (2007). “Implementation of shape memory alloy dampers for passive control of structures subjected to seismic excitations.” *Journal of Constructional Steel Research*, 63(12), 1570–1579.

Motahari, S. A., and Ghassemieh, M., (2007). “Multilinear one-dimensional shape memory material model for use in structural engineering applications.” *Engineering Structures*, 29(6), 904-913.

Namita, Y, Shigeta M, Yoshinaga T, Gotoh N and Kawahata, J., (1991). “The application of elasto-plastic support devices for a piping system.” *JSME International Journal Series. 3, Vibration, control engineering, engineering for industry*, 34(1), 42-49.

Osman, E. O. and Stefan, H., (2010). “Evaluation of the performance of a sliding-type base isolation system with a NiTi shape memory alloy device considering temperature effects.” *Engineering Structures*, 32(1), 238-249.

Ozbulut, O. E., Daghash, S., and Sherif, M. M., (2015). “Shape memory alloy cables for structural applications.” *Journal of Materials in Civil Engineering*, *28*(4), 401-517.

Ozbulut, O. E., and Hurlebaus, S., (2010). “Neuro-fuzzy modeling of temperature-and strain-rate-dependent behavior of NiTi shape memory alloys for seismic applications.” *Journal of Intelligent Material Systems and Structures*, 21(8), 837-849.

Park, Y. J, and Hofmayer C.H., (1995). “Practical application of equivalent linearization approaches to nonlinear piping systems.” *Seismic Engineering Conference Proceedings*. ASME PVP., vol 312, 187-200.

Parulekar, Y. M., Reddy, G. R., Vaze, K.K., Ghosh, A.K., Kushwaha, H.S., Ramesh Babu, R., (2009). “Seismic response analysis of R.C.C structure with yielding dampers using linearization techniques.” *Nuclear Engineering and Design*, 239 (12), 3054-3061.

Parulekar, Y.M., Reddy, G. R., Vaze, K.K., Kushwaha, H.S., (2003). "Elasto-plastic damper for passive control of seismic response of piping systems", *BARC Internal Report no. BARC/2003/E/028, Reactor Safety Division, BARC, Mumbai.*

Parulekar, Y.M., Reddy G. R, Vaze, K, K., and Kushwaha H. S., (2004). "Lead extrusion dampers for reducing seismic response of coolant channel assembly." *Nuclear Engineering and Design*, 227(2),175–183.

Parulekar, Y. M., Reddy, G. R., Vaze, K. K., Guha, S., Gupta, C., Muthumani, K., and Sreekala, R., (2012). "Seismic response attenuation of structures using shape memory alloy dampers." *Structural Control and Health Monitoring*, 19(1), 102-119.

Parulekar, Y.M, Reddy G. R, Vaze K.K., and Muthumani K., (2006). "Passive control of seismic response of piping systems." *Journal of Pressure Vessels Technology*, 128(3), 364-369.

Parulekar, Y. M., Kiran, A. R., Reddy, G. R., Singh, R. K., and Vaze, K. K., (2014). Shake table tests and analytical simulations of a steel structure with shape memory alloy dampers. *Smart materials and structures*, *23*(12), 125002.

Pujari, N. N., and Bakre, S. V., (2011). "Optimum placement of X-plate dampers for seismic response control of multi-storeyed buildings." *International Journal of Earth Sciences and Engineering*, 4 (6), 481-485.

Qian, H., Li, H., Song, G., and Guo, W., (2013). "Recentering shape memory alloy passive damper for structural vibration control." *Mathematical Problems in Engineering*, *2013*.

Qian, H., Li, H., and Song, G., (2016). "Experimental investigations of building structure with a superelastic shape memory alloy friction damper subject to seismic loads." *Smart Materials and Structures*, 25(12), 125-026.

Reddy, G. R., Suzuki K and Watanabe T., (1999). "Linearization techniques for seismic analysis of piping system on friction support." *Journal of Pressure Vessel Technology*, 121,103-108.

Reedlunn, B., Daly, S., and Shaw, J., (2013). “Superelastic shape memory alloy cables: Part I–isothermal tension experiments.” *International Journal of Solids and Structures*, *50*(20-21), 3009-3026.

Ren, W., Li, H., and Song, G., (2007). “Phenomenological modeling of the cyclic behavior of superelastic shape memory alloys.” *Smart materials and structures*, *16*(4), 1083.

Russell, E., Jamie, E. P., and Reginald, D., (2010). “Experimental response modification of a four-span bridge retrofit with shape memory alloys.” *Structural Control Health Monitoring*,17(6), 694–708.

Saadat, S., Salichs, J., Noori, M., Hou, Z., Davoodi, H., Baron, I., Suzuki, Y., and Masuda, A., (2002). “An overview of vibration and seismic applications of NiTi shape memory alloy.” *Smart Materials and Structures*, 11(2), 218–229.

Sathish Kumar, K., Muthumani, K., Gopalakrishnan, N and Sivarama Sarma, B., (2003). “Reduction of large seismic deformations using elasto-plastic passive energy dissipaters.” *Defence Science Journal*, 53(1), 95-103.

Sharabash, A. M., and Andrawes, B. O., (2009). “Application of shape memory alloy dampers in the seismic control of cable-stayed bridges.” *Engineering Structures*, 31(2), 607-616.

Shinozuka, M., Chaudhuri, S. R., Mishra, S. K., (2015). “Shape-memory-alloy supplemented lead rubber bearing (SMA-LRB) for seismic isolation.” *Probabilistic Engineering Mechanics*, 41, 34-45.

Song, G., Li, H. and Qian, H., (2008)., “Experimental and analytical investigation on innovative hybrid shape memory alloys dampers for structural control, active and passive smart structures and integrated systems.” *Proc. of SPIE*, 6928, 277-786.

Soong, T. T. and Dargush G. F., (1997). “Passive energy dissipation system in structural engineering.” Wiley, New York.

Soong, T. T. and Spencer, Jr., B. F., (2002). “Supplemental energy dissipation: state-of-the-art and state-of-the practice.” *Engineering Structures*, 24 (3), 243-259.

Soong, T.T., (1990). “Active structural control: theory and practice.” Longman, England and Wiley, New York, NY.

Spencer, Jr., B. F., and Nagarajaiah, S., (2003). “State of the art of structural control, *Journal of Structural Engineering*.” 129 (7), 845-856.

Symans, M. D., and Constantinou, M. C., (1999). “Semi-active control system for seismic protection of structures a state-of-the art review.” *Engineering Structures*, 21 (6), 469-487.

Tamai, H., and Kitagawa, Y., (2002). “Pseudoelastic behavior of shape memory alloy wire and its application to seismic resistance member for building.” *Computational Materials Science*, *25*(1-2), 218-227.

Tanaka, K., (1986). “Thermo-mechanical sketch of shape memory effect: One dimensional tensile behaviour.” *Res. Mechanica*.,18(3), 251-263.

Tobushi, H., Shimeno, Y., Hachisuka, T., and Tanaka, K., (1998). “Influence of strain rate on superelastic properties of TiNi shape memory alloy.” *Mechanics of Materials*, *30*(2), 141-150.

Tsai, K.C., Chen, H.W., Hong, C.P., and Su, Y.F., (1993). “Design of steel triangular plate energy absorbers for seismic-resistant construction.” *Journal of Earthquake Spectra* 9(3), 505-528.

Tsai, C.S., and Tsai K.C., (1995) “TPEA device as seismic damper for high rise buildings.” *Journal of Engineering Mechanics*, 121(10), 1075-1081.

Tehranizadeh, M., (2001). “Passive energy dissipation device for typical steel frame building in Iran.” *Engineering Structures*, 23(6), 643–655.

Tena-Colunga, A., (1997). “Mathematical modelling of the ADAS energy dissipation device.” *Engineering Structures*, 19(10), 811–821.

Toopchi-Nezhad, H., Love, J. S., and Tait, M. J., (2011). “A hybrid structural control system using a tuned liquid damper to reduce the wind induced motion of a base isolated structure.” *Engineering Structures*, *33*(3), 738-746.

Torra, V., Isalgue, A., Martorell, F., Terriault, P., and Lovey, F.C., (2007). “Built in dampers for family homes via SMA: an ANSYS computation scheme based on mesoscopic and microscopic experimental analyses.” *Engineering Structures*, 29(8), 1889–1902.

Wang, C. H., Yan, W., Zhang, X. P., and Mai, Y. W., (2003). “Theoretical modelling of the effect of plasticity on reverse transformation in superelastic shape memory alloys.” *Materials Science and Engineering 354*(1-2), 146-157.

Wang, W., Hong T, Shao L., and Chen Y., (2016). “Cyclic behavior of connections equipped with NiTi shape memory alloy and steel tendons between H-shaped beam to CHS column.” *Engineering Structures*, 88, 37–50.

Wen, Y.K., (1980) “Equivalent linearization for hysteretic systems under random excitation.” *Journal of Applied Mechanics,* 47,150–154.

Whittaker, S., Bertero V. V., Thompson C.L., and Alonso L.J., (1991). “Seismic testing of steel plate energy dissipation devices.” *Earthquake Spectra*, 7(4), 563-604.

Whittaker, S, V.V., Bertero, L.J., and Alonsoand, C.L., (1989). “Earthquake simulator testing of steel plate added damping and stiffness elements.” Report UCB/EERC-89/02, *Earthquake Engineering Research Center, University of California at Berkeley*.

Wilde, K., Gardoni, P, and Fujino, Y., (2000). “Base isolation system with shape memory alloy device for elevated highway bridges.” *Engineering Structures*, 22(3), 222–229.

Wilson, J. C., and Wesolowsky, M. J., (2005). "Shape memory alloys for seismic response modification: a state-of-the-art review." *Earthquake Spectra*, 21(2), 569-601.

Wilson, J. C., and Wesolowsky, M. Design and Performance of isolators with Shape memory alloys., (2013) *Proceedings of 15th World Conference of Earthquake*

Engineering, New Zealand Society for earthquake engineering McMaster University, Hamilton, ON., Canada,

Wolons, D., Gandhi, F., and Malovrh, B., (1998). "Experimental investigation of the pseudoelastic hysteresis damping characteristics of shape memory alloy wires." *Journal of Intelligent Material Systems and Structures*, *9*(2), 116-126.

Xia, R.D., Hanson and Su, Y.F., (1992). "Design of supplemental steel damping devices for buildings." *Proceedings of 10th World Conference of Earthquake Engineering*, Madrid, Spain, 4139–4142.

Yang, C. W., DesRoches, R., and Roberto, T. L., (2010). "Design and analysis of braced frames with shape memory alloy and energy-absorbing hybrid devices." *Engineering Structures*, 32(2), 498-507.

Yu-Lin, H. L., Ai-Qun, Q. S. L., Leung, A. Y. T. and Ping-Hua, L., (2003). "Structural vibration control by shape memory alloy damper." *Earthquake Engineering and Structural Dynamics*, 32(3), 483–494.

Zhang, Y. P., Li, D. S., and Zhang, X. P., (2007). "Gradient porosity and large pore size NiTi shape memory alloys. *Scripta Materialia*," *57*(11), 1020-1023.

Zhu, S., and Zhang, Y., (2007). "Seismic analysis of concentrically braced frame systems with self-centering friction damping braces." *Journal of Structural Engineering*, 134(1), 121-31.

Zhang, Y., and Zhu, S., (2008). "Seismic response control of building structures with superelastic shape memory alloy wire dampers". *Journal of Engineering Mechanics*, *134*(3), 240-251.

LIST OF PUBLICATIONS

- U. Vajreshwari, K. Venkataramana, G. R. Reddy, V. Rajeev (2013), "Application of the Dampers for Vibration Control of Structure: An Overview," *International Journal of Research in Engineering and Technology* (IJRET), Vol. 2, No.1, November 2013, ISSN:2321-7308.
- Vajreshwari Umachagi, Manasa Bhat K.I, Katta Venkataramana, (2015), "Applications of shape memory alloy devices in vibration control of structures", *Proc. of 4th International Engineering Symposium, March 4-6, 2015, Kumamoto University, Japan, Paper No. C2-5-1, pp.C51-C56.*
- U. Vajreshwari and K. Venkataramana (2019), "X plate damper for seismic control of the building." *International Journal of Water Resource Engineering and Management* (IJWRE) Vol 6, No.1, March 2019, ISSN:2349-4336
- U. Vajreshwari and K. Venkataramana (2019), "Seismic performance of RC building using SMA device" *International Journal of Structural Engineering and Analysis* (IJSEA), Vol 5, No.1, May 2019, ISSN:2456-5326.

BIO DATA

Name : VAJRESHWARI UMACHAGI

Contact No. : +91-9482320979

E-Mail : vmumachagi@gmail.com

Gender : FEMALE

Native place : Belgaum Galli, Hubli-580028

Educational Qualifications

Degree	College/University	University	Percentage	Year of Passing
Ph.D. (Structural Engineering)	National Institute of Technology Karnataka, Surathkal-575025, Karnataka	National Institute of Technology Karnataka, Surathkal-575025, Karnataka	8.5 (CGPI)	2012-On going
M.Tech (Computer aided design of Structures)	S.D.M College of Engineering and Technology, Dharwad-580002, Karnataka	Visvesvaraya Technological University, Belgaum-590018, Karnataka	79.91%	2010-2011
B. E	S.D.M College of Engineering and Technology, Dharwad-580002, Karnataka	Visvesvaraya Technological University, Belgaum-590018, Karnataka	64.54%	2005-2009

PUBLICATIONS

1) U. Vajreshwari and K. Venkataramana (2019), “X-plate damper for seismic control of the building.” *International Journal of Water Resource Engineering and Management* (IJWRE) Vol 6, No.1, March 2019, ISSN:2349-4336.

2) U. Vajreshwari and K. Venkataramana (2019), “Seismic performance of RC building using SMA device” *International Journal of Structural Engineering and Analysis* (IJSEA), Vol 5, No.1, May 2019, ISSN:2456-5326.

3) Vajreshwari Umachagi, Manasa Bhat K.I, Katta Venkataramana, (2015), “Applications of shape memory alloy devices in vibration control of structures”, *Proc. of 4th International Engineering Symposium, March 4-6, 2015, Kumamoto University, Japan, Paper No. C2-5-1, pp.C51-C56.*

4) U. Vajreshwari, K. Venkataramana, G. R. Reddy, V. Rajeev (2013), "Application of the Dampers for Vibration Control of Structure: An Overview," *International Journal of Research in Engineering and Technology* (IJRET), Vol. 2, No.1, November 2013, ISSN:2321-7308.

5) Vajreshwari Umachagi, R.J. Fernandes., S.B. Vanakudre., “Optimization of Antisymmetric Angle Ply Laminated Composite Plates by HSDT using Genetic Algorithm”, *International Journal of Earth Science and Engineering*, Vol 4, No.6, October, 2011, 476-480.

Experience and Training:

- Teaching assistant in NITK, Surathkal, Lab and subjects: Design and drawing of steel structures, Concrete and Highway Material Lab and Cad Lab during July 2012 to July 2016 in the Dept. of Civil Engineering.
- Assistant Professor in S.D.M College of Engineering and Technology, Dharwad during August 2011 to July 2012 in the Dept. of Civil Engineering.
- Participated in a three days' workshop on "Advanced Course on Seismic Response Control and Damage Mitigation Methodologies for Building and Structures" during Feb 19th to 21st Feb 2014, in CSIR campus, CSIR road, Taramani, Chennai -600113, India.
- Participated in a two days' workshop on Civil Infrastructure and Structural Materials during July 28th and 29th 2014, sponsored by TEQIP II, in NITK, Surathkal, Mangalore 575025, India
- Participated in two days' workshop on Faculty development program on Civil FEM, organized by VTU, in March 2012 Belgaum and certified.
- Participated in a three days' workshop on "Earthquake Resistant Design and Construction" in May 2010 B.V.B.C.E.T, Hubli and certified.